*Evolution*, 2026, **80**(6), 1311–1328
https://doi.org/10.1093/evolut/qpag062
Advance access publication 21 April 2026
**Original Article**

# Phenotypic crypticity despite strong phylogenetic divergence: diversification dynamics in a species complex of Arabian *Pristurus* geckos

**Thore Koppetsch[1], Bernat Burriel-Carranza[2,3], Elizabeth Glynne[4], Benjamin Wipfler[5], Xiao-Zhu Luo[5,6], Arild Johnsen[1], Dean C. Adams[4], Salvador Carranza[2], Michael Matschiner[1,7]**

[1]Natural History Museum, University of Oslo, Oslo, Norway
[2]Institute of Evolutionary Biology (CSIC-Universitat Pompeu Fabra), Barcelona, Spain
[3]Museu de Ciències Naturals de Barcelona, Barcelona, Spain
[4]Iowa State University, Ames, Iowa, United States
[5]Museum Koenig, Leibniz Institute for the Analysis of Biodiversity Change, Bonn, Germany
[6]Department of Entomology, College of Plant Protection, South China Agricultural University, Guangzhou, China
[7]Faculty of Biology, Ludwig Maximilian University Munich, Planegg, Germany

Corresponding author: Natural History Museum, University of Oslo, Blindern, P.O. Box 1172, 0138 Oslo, Norway. Email: thore.koppetsch@nhm.uio.no

## Abstract

Absence of phenotypic differentiation can challenge the study of diversification by concealing evolutionary divergence through morphological similarity. Such cryptic species diversity is found particularly often in extreme environments, including arid mountain ranges. In the Hajar Mountains of southeastern Arabia, the *Pristurus rupestris* species complex comprises divergent lineages with notable phenotypic variation. Here, we investigate the evolutionary dynamics of this radiation by integrating geometric morphometric analyses with whole-genome sequencing and phylogenomic reconstructions. We analyzed five species—*P. ali*, *P. assareen*, *P. feulneri*, *P. omanensis*, and *P. rupestris*—including all previously identified genetic lineages within those species, and generated a new reference genome for an Old World sphaerodactylid gecko (*P. rupestris* sensu stricto). Morphometric analyses of comprehensive two- and three-dimensional morphological datasets indicate strong overlap in both body and head shape. Despite considerable phenotypic similarities, our results reveal deep interspecific divergences exceeding 16 million years and contrasting demographic histories. While we detected introgression restricted to specific lineage pairs, phenotypic crypticity persists across the entire complex, suggesting stabilizing selection in harsh environments. Our study highlights the *P. rupestris* species complex as an ideal model for investigating the role of environmental constraints in limiting morphological divergence and shaping diversification dynamics in arid mountain ecosystems.

**Keywords:** cryptic species, geckos, divergence, phenotypic similarity, morphological stasis, phylogenomics

## Introduction

Diversification of lineages accompanied by pronounced morphological differentiation includes some of the most spectacular examples of evolution in action. This pattern, classically exemplified by so-called adaptive radiations, has long shaped our intuition that lineage divergence is typically coupled with ecological and phenotypic divergence. Yet comparative studies demonstrate that rates of lineage diversification and morphological evolution can be markedly decoupled (Adams et al., 2009). While adaptive radiations are often characterized by rapid bursts of morphological disparity (García-Navas et al., 2018; Warheit et al., 1999), other clades diversify with little or no obvious phenotypic change, revealing that evolutionary branching does not necessarily entail phenotypic innovation and may instead result in patterns consistent with nonadaptive radiations. Lineages that exhibit pronounced genetic structure but minimal observable morphological differentiation are commonly described as cryptic species (Bickford et al., 2007; Jörger & Schrödl, 2013; Struck et al., 2018). While such apparent crypticity can partly reflect the limits of morphological diagnosis, it should not be treated merely as a taxonomic inconvenience, but as a window into the processes governing morphological evolution, lineage cohesion, and speciation. At a broader scale, cryptic species are now recognized as widespread across vertebrates, and because many lineages remain formally undescribed, accounting for cryptic diversity is critical to accurately estimate species richness, speciation and extinction rates, and diversification dynamics, as well as to inform conservation measures (Zhang & Wiens, 2026). For example, Chan et al. (2026) demonstrated that cryptic diversity can be shaped by gene flow, particularly for lineages diversifying within the "gray zone" of speciation, where divergence and cohesion interact over extended periods of time. Consistent with this, recently diverged species often exhibit minimal phenotypic differences when there is significant ecological overlap (Gabaldón et al., 2013; Scriven et al., 2016). Still, it is intriguing that phenotypes can also

Received October 1, 2025; revisions received March 20, 2026; accepted March 27, 2026
Associate Editor: Antigoni Kaliontzopoulou; Handling Editor: Hélène Morlon
© The Author(s) 2026. Published by Oxford University Press on behalf of The Society for the Study of Evolution (SSE). This is an Open Access article distributed under the terms of the Creative Commons Attribution License (https://creativecommons.org/licenses/by/4.0/), which permits unrestricted reuse, distribution, and reproduction in any medium, provided the original work is properly cited.

Downloaded from https://academic.oup.com/evolut/article/80/6/1311/8660089 by guest on 08 June 2026

remain strikingly similar over long evolutionary time, a pattern that has often been suggested to result from a lack of ecological opportunity (Losos & Mahler, 2010; Meier et al., 2019; Stroud & Losos, 2016; Wellborn & Langerhans, 2015). Facing global biodiversity loss (Butchart et al., 2010), it is crucial to both identify undescribed species and understand factors driving crypticity. Struck et al. (2018) identified recent divergence, parallelism, convergence, and stasis as the main evolutionary processes shaping cryptic species, highlighting the disparity between morphological distinctness and genetic divergence—a framework applicable also to empirical systems (Schembri et al., 2025).

Extreme environments provide powerful natural laboratories for investigating these dynamics. Strong and consistent selective pressures can promote phenotypic convergence among distantly related taxa, e.g., in poeciliid fishes adapted to sulfidic springs (Tobler et al., 2011) or in subterranean amphipods (Delić et al., 2025; Lefébure et al., 2006). Conversely, morphological stasis despite genetic divergence also occurs in deep-sea taxa (Brandt et al., 2014; Brasier et al., 2016; Etter et al., 1999; Vrijenhoek et al., 1994), and, strikingly, in sympatric interstitial *Stygocapitella* annelids that diverged about 140 million years ago (mya) (Cerca et al., 2020). Among terrestrial biomes, arid and semi-arid regions—covering one-third of Earth's land—harbor unique and understudied biodiversity shaped by extreme conditions (Brito et al., 2014; Durant et al., 2012; Šmíd et al., 2021). Considerable cryptic diversity has been documented in desert taxa worldwide, including Saharan rodents (Boratynski et al., 2012), Australian tiger beetles (López-López et al., 2016), Central Asian scorpions (Graham et al., 2019), and Californian beetles (Rubinoff et al., 2020). Squamate reptiles are particularly diverse in arid and semi-arid regions (Cox & Cox, 2015; Pianka, 1989; Roll et al., 2017; Šmíd et al., 2021; Tejero-Cicuéndez et al., 2022), with cryptic lineages reported in agamids, lacertids, skinks, snakes, and especially geckos (Agarwal et al., 2014; Barata et al., 2012; Burriel-Carranza et al., 2025a; Carter et al., 2025; Garcia-Porta et al., 2017; McDonald et al., 2024; Mendes et al., 2018; Prates et al., 2024; Schield et al., 2018; Simó-Riudalbas et al., 2017, 2018; Smith et al., 2011; Tamar et al., 2019a, 2019b).

The Hajar Mountains in southeastern Arabia exemplify diversification in arid mountain systems, with up to 49 squamate lineages identified (Burriel-Carranza et al., 2025b). This ~600 km mountain range, originating ~40 mya (~90 mya for proto-Hajars, Hansman et al., 2017), is divided into Western, Central, and Eastern Hajars, with the Central Hajars reaching over 3,000 m above sea level (masl). Isolated by the Rub Al Khali desert and northern coastal plains, this old and complex mountain system is a hotspot of endemicity in Arabia—particularly for squamates—harboring 23 endemic reptile species (Burriel-Carranza et al., 2025b).

Geckos dominate this endemicity (19 species) with the families Gekkonidae (genera *Hemidactylus* and *Trachydactylus*), Phyllodactylidae (genera *Asaccus* and *Ptyodactylus*), and Sphaerodactylidae (genus *Pristurus*) (Burriel-Carranza et al., 2022; Carranza et al., 2021). Particularly the genus *Pristurus*, also known as "semaphore geckos," includes extensive cryptic diversity (Burriel-Carranza et al., 2025a; Garcia-Porta et al., 2017). With 32 described species (Uetz et al., 2025) across Africa, Arabia, Socotra, and the Persian Gulf, they display strong ecological specialization and body size disparity, making them an excellent system for studying diversification dynamics (Arnold, 1993, 2009; Garcia-Porta et al., 2016, 2017; Tejero-Cicuéndez et al., 2021, 2023).

In the Hajar Mountains, a remarkable radiation is the *Pristurus rupestris* Blanford, 1874, species complex, once considered a single widespread taxon (Arnold, 2009). Phylogenetics later revealed multiple, independently evolving lineages (Badiane et al., 2014). One major clade, distributed along the western and southern coast of the Arabian Peninsula, was subsequently recognized as *Pristurus guweirensis* Haas, 1943, one of the most abundant species in its genus (Burriel-Carranza et al., 2023b). In contrast, another clade represents a cryptic species complex within the southeastern Arabian *P. rupestris* group. Molecular analyses using Bayes factor delimitation (BFD) identified 12 deeply divergent lineages within this group, highlighting its considerable genetic diversity (Burriel-Carranza et al., 2025b). A recent integrative taxonomic revision of the systematically challenging *P. rupestris* species complex identified four new cryptic species: *P. ali* Burriel-Carranza, Koppetsch, Garcia-Porta & Carranza, 2025, *P. assareen* Burriel-Carranza, Koppetsch, Garcia-Porta & Carranza, 2025, *P. feulneri* Burriel-Carranza, Koppetsch, Garcia-Porta, Els & Carranza, 2025, *P. omanensis* Burriel-Carranza, Koppetsch, Garcia-Porta & Carranza, 2025 (Burriel-Carranza et al., 2025a). While Garcia-Porta et al. (2017) found support for morphological segregation within the *P. rupestris* species complex with both a "robust" and "slender" phenotype, more detailed analyses using a comprehensive morphological characterization based on linear measurements revealed a high degree of phenotypic overlap and strong crypsis for the four species listed above and *P. rupestris* sensu stricto (s. strc.) (Burriel-Carranza et al., 2025a). Despite all species occurring sympatrically with at least one other representative of the species complex, ddRADseq data analyses of genome-wide SNPs did not indicate ongoing genetic exchange among the species (Burriel-Carranza et al., 2025a).

The lack of clear morphological differentiation despite deep divergence makes the *P. rupestris* complex a powerful system for studying cryptic diversification in arid mountains. Although linear measurements show strong interspecific overlap and broad intraspecific variation, it remains unclear whether some species possess subtle anatomical traits indicating ecological segregation despite sympatry. Particularly, head shape is linked to various ecologically adaptive traits, e.g., diet, habitat use, locomotion, or behavior in different lizard taxa (Herrel et al., 2001; Kaliontzopoulou et al., 2012, 2015; Openshaw & Keogh, 2014; Verwaijen et al., 2002). It is also unclear whether phenotypic crypticity in these *Pristurus* geckos is shaped by similar extreme environmental conditions, or rather by similar demographic histories or genetic exchange. While ddRADseq data analyses based on a limited number of genome-wide SNPs recovered unique evolutionary units within the *P. rupestris* complex (Burriel-Carranza et al., 2025a), in-depth analyses of demographic history, genetic diversity or recent and ancient genetic exchange requiring more complete genomic data are still missing. More reliable divergence time estimates are needed to clarify separation among deeply divergent lineages, as shown in other Hajar Mountains geckos, e.g., *Asaccus caudivolvulus* Arnold & Gardner, 1994 (Burriel-Carranza et al., 2024).

Downloaded from https://academic.oup.com/evolut/article/80/6/1311/8660089 by guest on 08 June 2026

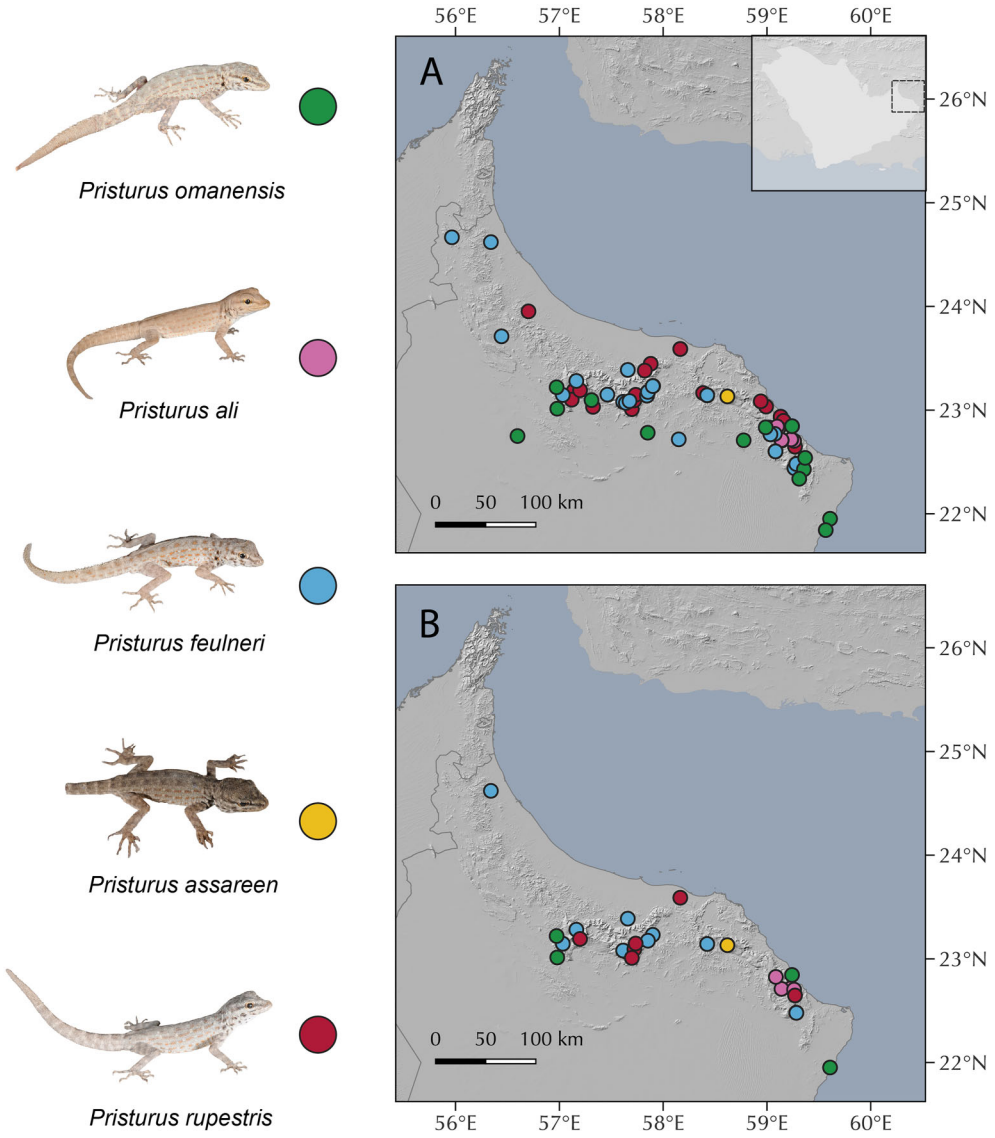



**Figure 1.** Geographic map showing the distribution of the species of the *Pristurus rupestris* species complex and the origin of the specimens used for (A) morphological and (B) phylogenomic analyses. Photos on the left depict single representatives of the five *Pristurus* species.

Here, we present an integrative analysis of the diversification dynamics of the extraordinary radiation of *Pristurus* geckos in the Hajar Mountains, using comprehensive two- and three-dimensional morphological datasets in parallel with whole genome sequencing (WGS) data. In addition to linear measurements, we obtained μ-computed tomography (μ-CT) scans for 84 individuals covering all the five species and 12 genetic lineages of the *P. rupestris* species complex (Figure 1), and explored the phenotypic variation in this group using a geometric morphometric approach. We assembled a reference genome for *P. rupestris* and generated WGS data for 28 specimens of the entire radiation, as well as two individuals of the sister species *P. flavipunctatus* Rüppell, 1835. Using the comprehensive genomic dataset, we performed a range of analyses to investigate the divergence, the role of ongoing and ancient hybridization, and the demographic history of the entire *P. rupestris* species complex. Building on previous systematic work (Burriel-Carranza et al., 2025a), we move beyond species delimitation by studying associations of morphological traits in the context of the radiation's dynamic evolutionary past to evaluate the phenotypic crypticity in this group. With our in-depth analyses of both phenotypic and genomic data, we highlight the importance of an integrative framework to understand the identity and origin of intricate species complexes.

## Materials and methods

### Specimens

In this study, we use a combination of phenotypic and molecular data to characterize the diversification dynamics of the *P. rupestris* species complex. All specimens used in this study were collected between 2005 and 2022. Vouchers were preserved in 99% ethanol and stored at −20 °C. Tail tips were taken from the specimens used for WGS and stored in 99% ethanol at −20 °C prior to DNA extraction. Specimens were collected and manipulated with the authorization and under strict control and permission of the government of Oman (Environment Authority), who issued all the necessary collecting and export permits for this study (Refs: 08/2005;

Downloaded from https://academic.oup.com/evolut/article/80/6/1311/8660089 by guest on 08 June 2026

16/2008; 38/2010; 12/2011; 13/2013; 21/2013; 37/2014; 601 31/2016; 6210/10/21). Specimens were captured and processed following the guidelines and protocols stated in the collecting permits and agreements obtained from the competent authorities of Oman. As a result of the characteristics of this study and the total control and compliance with the laws, regulations, and procedures of this kind of biodiversity study in Oman, it did not need the approval of an Institutional Animal Care and Use Committee (IACUC) or ethics committee.

For the morphological characterization, 84 specimens were selected representing all species of the *P. rupestris* species complex, including all the genetic lineages ("BFD1" to "BFD12") identified by Burriel-Carranza et al. (2025a) (Figure 1; Table S1). Additionally, 28 specimens selected for the molecular analyses in the present work comprise the entire radiation of the *P. rupestris* species complex: 4 individuals of *Pristurus ali* (all of BFD4), 2 *P. assareen* (all of BFD12), 12 *P. feulneri* (2 of BFD7, BFD8, BFD9, BFD11, respectively; 4 of BFD10), 4 *P. omanensis* (2 of BFD5 and BFD6 respectively), 6 of *P. rupestris* s. strc. (2 of BFD1, BFD2, and BFD3, respectively). In addition, two individuals of the sister species of *P. rupestris*, *P. flavipunctatus*, were chosen as an outgroup (Table S2). The specimen used for the reference genome assembly for *P. rupestris* s. strc. was collected on 24 February 2022 and originated from the type locality in Muscat, Oman (Table S2).

## Morphological data

### Linear measurements and μ-CT

For a morphological characterization, we obtained nine linear measurements from 84 *Pristurus* specimens representing all lineages within the *P. rupestris* complex (Table S1). Characters were partially selected from previous taxonomic and morphological analyses of *Pristurus* geckos (Burriel-Carranza et al., 2025a; Garcia-Porta et al., 2017). All measurements were taken by T.K. using a Vernier caliper to the nearest 0.1 mm. For all specimens, sex and the following meristic characters were determined: snout-vent length (SVL, snout to the cloaca); trunk length (TrL, distance between the internal parts of fore and hind limb insertions); head length (HL, snout to anterior-most point of ear opening); head height (HH, laterally at anterior-most point of ear opening); head width (HW, at anterior-most point of ear opening); humerus length (LHu, from elbow to forelimb insertion); ulna length (LUn, from wrist to elbow); femur length (LFe, from knee to hindlimb insertion); and tibia length (LTb, from ankle to knee).

To study osteological morphology, each specimen was scanned with a Skyscan 1173 μ-CT (Bruker, Billerica/USA) at the Museum Koenig in Bonn, Germany. The specimens were firmly positioned individually and fixed with foam in 70% EtOH-filled tubes, which were glued on a stub before scanning. Scans were performed with the following parameters: voltage: 49 kV; current: 133 μA; rotation steps: over 360°–0.21°; exposure time: 850 ms; image pixel size: 18.1 μm; frame averaging: 6; random movement: 15. All scans are part of the digital collection of the Museum Koenig (LIB) and can be obtained from T.K. or B.W. Scans were reconstructed with NRecon (Bruker, Billerica/USA), imported into Amira v.6.1.2 (Thermofisher) for skull separation, and volume-rendered in VG Studio 3.3 (Volume Graphics). Three-dimensional skull models were exported in ASCII polygon (.ply) format.

### Comparative phenotypic and statistical analyses

To explore body shape in the *P. rupestris* species complex, linear morphometric analyses were conducted on a set of log-transformed body measurements of 83 specimens of the *P. rupestris* species complex (the singleton of *P. assareen* was excluded from the analysis) (Table S1). Size effects were removed via regression on SVL. Because sexual dimorphism in SVL and the evaluated shape variables have been shown to be negligible in the *Pristurus rupestris* species complex (Garcia-Porta et al., 2017), we combined males and females in all subsequent analyses and did not include sex as a factor.

To capture the head shape of the 83 *Pristurus* skull models, we prepared a 3D-landmarking scheme consisting of 15 fixed landmarks, and 24 sliding semilandmarks on equidistant curves (Figure S1 and Table S3). The Stratovan Checkpoint software (Stratovan Corporation) was used to place and digitize fixed landmarks at specified osteological traits, as well as gliding semilandmarks to capture the shape and size of the eyes and orbits. Definitions and descriptions of the landmarking scheme are provided in Table S3. Landmark data were analyzed in R v.4.2.3 using geometric morphometrics (Adams et al., 2013). First, missing landmarks were estimated using the thin-plate spline (TPS) interpolation (see sensu: Bookstein et al., 1999; Gunz et al., 2009). Next, a generalized Procrustes analysis (GPA) was used to align the landmark configurations and remove nonshape information, including size. During this procedure, semilandmarks were slid along their respective curves to minimize bending energy, and symmetry was assessed using a predefined symmetry landmark matrix to extract symmetric shape components. Upon superimposition, shape variables were generated from the final configurations of all 3D-landmarks via orthogonal projection to tangent space. All morphometric analyses were performed using *geomorph* v.4.0.1 (Adams et al., 2021; Baken et al., 2021). Specimen information and associated environmental data were imported from a compiled dataset (Table S1). One species, *P. assareen*, was excluded from this analysis because it was represented by only a single specimen.

For statistical analyses of both body shape based on linear measurements and head shape based on 3D geometric morphometrics, principal component analyses (PCA) were used to explore patterns of shape variation across species, genetic lineages, elevation groups (high elevation >1,500 masl; low elevation <1,500 masl), and geographic regions (categorized as Western, Central, and Eastern Hajars) as defined in Burriel-Carranza et al. (2025b). To formally test for morphological differences, type-2 Procrustes analyses of variance (ANOVA) (function *procD.lm*; Baken et al., 2021) were performed separately on both body shape and head shape data using a linear model framework. Significance was assessed using distributions obtained from a resampling of 1,000 permutations using *geomorph* v.4.0.1 (Adams et al., 2021; Baken et al., 2021). Pairwise statistical comparisons were then conducted to evaluate differences in shape means between candidate species using *RRPP* (Collyer & Adams, 2018, 2023). To account for multiple testing, pairwise comparisons were assessed using a *p*-value of 0.05, and variance was evaluated using permutation-based statistical tests.

Downloaded from https://academic.oup.com/evolut/article/80/6/1311/8660089 by guest on 08 June 2026

For head shape only, a trajectory analysis was performed to assess patterns of cranial shape variation across species and elevation groups (Collyer & Adams, 2013). Differences in mean shape trajectories, trajectory convergence, and shape disparity were evaluated using permutation-based statistical tests. Cranial shape variation was visualized by predicting extreme shapes along the first two principal components using *shape.predictor()* (Baken et al., 2021). Shape deformations were illustrated with *plotRefToTarget()* (Baken et al., 2021), and a representative specimen was used for 3D mesh warping. To account for asymmetry, visualizations were generated using a symmetric reference shape. A phylomorphospace was constructed using *gm.prcomp()* (Baken et al., 2021), onto which we mapped the time-calibrated Bayesian individual-level phylogeny (including all 83 specimens) from Burriel-Carranza et al. (2025b) (publicly available from the Dryad Digital Repository (https://doi.org/10.5061/dryad.r7sqv9sj3; file: Trees/Calibrated_BI_Gene_trees/07Prup.tree) and originally presented in their Figure S18). This tree includes all individuals incorporated in the morphometric analyses and thus allows direct specimen-level mapping.

## Molecular data

### DNA extraction, library preparation, and sequencing

We extracted high molecular weight genomic DNA from tail tips of 30 individuals of the specimens listed in Table S2. We followed the manufacturer's protocol of the MagAttract HMW Kit (Qiagen) and sequenced a total of 30 Illumina libraries, aiming for a coverage of ~15× in paired-end reads (150 bp) on a NovaSeq6000 lane. Sequencing was conducted by Novogene Co. High molecular weight DNA for the reference genome assembly was obtained from muscle tissue of a *Pristurus rupestris* s. strc. specimen (Table S2), following the same protocol as above. Long-read data were obtained for this specimen through PacBio HiFi sequencing aiming for a 60× coverage.

### Genome assembly

The reference genome was assembled using Hifiasm v.0.18.2 (Cheng et al., 2021). Quality assessment and general metrics for the HiFi assembly were carried out with QUAST v.5.0.2 (Gurevich et al., 2013), while Merqury v.1.3 (Rhie et al., 2020) was used to evaluate base quality and k-mer completeness. BUSCO+ v.5.5.0 (Manni et al., 2021) was used for assessing completeness, and HiFi reads were aligned to the assembly with Minimap2 v.2.17 (Li, 2018), followed by processing with SAMtools v.1.10 (Li et al., 2009). The BUSCO scores and read coverage were analyzed with BlobToolKit v.3.1.4 (Challis et al., 2020), and contamination was assessed using a local NCBI database, identifying and discarding putative contaminations with BLAST+ v.2.13.0 (Boratyn et al., 2013). Purge dups (Guan et al., 2020) was used to remove potential duplicates from the primary assembly. The k-mer distribution ($k = 21$) was generated using Jellyfish v.2.3 (Marçais & Kingsford, 2011). SmudgePlot v.0.2.4 and GenomeScope v.2.0 (Ranallo-Benavidez et al., 2020) were used to assess genome ploidy, size, repetitiveness, and heterozygosity.

### Processing of WGS data

Raw Illumina reads of 30 individuals were preprocessed with fastp v.0.23.2 (Chen et al., 2018) for adapter and polyG trimming, quality filtering (Phred ≧ Q15), and removal of reads <30 bp. Contigs <20 kb were discarded before mapping. The reference genome was indexed with BWA v.0.7.17 (Li, 2013), and reads were mapped using bwa-mem2 (Vasimuddin et al., 2019). Resulting BAM files were indexed with SAMtools v.1.17 and duplicates marked with Picard v.2.26.10 (https://broadinstitute.github.io/picard/). A mappability mask was generated using overlapping 100 bp fragments mapped back to the reference, excluding sites where <95% of fragments mapped perfectly, using the program SEQBILITY (https://github.com/lh3/misc) and following the SNPable pipeline (http://lh3lh3.users.sourceforge.net/snpable.shtml). Mapping statistics were obtained with SAMtools v.1.12 (Li et al., 2009), coverage with Mosdepth (Pedersen & Quinlan, 2018), and quality control with Qualimap (García-Alcalde et al., 2012). Variants were called with GATK's "HaplotypeCaller" and "GenotypeGVCFs" (GATK v.4.4.0.0; McKenna et al., 2010) and summarized with BCFtools v.1.17 (Li, 2011). Genome soft-masking was performed using Red (Repeat Detector) (https://github.com/nextgenusfs/redmask).

To ensure high call reliability, we applied strict variant filtering using BCFtools v.1.15.1 (Li, 2011). Monomorphic sites were removed, and low-quality genotypes (FMT/DP <4, FMT/GQ <20) were set to "missing." Sites were discarded if they failed thresholds for strand bias (FS > 20), normalized quality (<2), RMS mapping quality (<30), read depth (<150 or >300), positional/mapping bias (MWU<−0.5), inbreeding coefficient (<−0.5), or strand odds ratio (>3). Indels were normalized and sites without reference alleles removed. Low minor allele count indels (<2) were filtered with *make_indel_mask.rb* (Ronco et al., 2021), and both the mappability and repeat masks applied. Spanning deletions were replaced with missing data using *replace_spanning_deletions.rb* (Ronco et al., 2021), and sites no longer polymorphic were removed. Missingness per site was calculated with BCFtools, and sites with >50% missing data were excluded. Filtered scaffolds were concatenated with GATK's "GatherVCFs" (McKenna et al., 2010), producing the "permissive dataset" of 86,977,236 SNPs. A more stringent "strict dataset" applied similar filtering but with FMT/DP < 5, FMT/GQ < 25, FS > 15, RMS mapping quality <40, and strand odds ratio >2, resulting in 2,098,690 SNPs.

### Phylogenomic analyses

To investigate the divergences and relationships within the *Pristurus* radiation of the Hajar Mountains, we conducted phylogenomic reconstructions using the "strict dataset" of genome-wide nuclear SNPs. We assigned the individuals to the respective genetic lineages defined by Burriel-Carranza et al. (2025b) and defined *P. flavipunctatus* as sister to all other species to construct a time-calibrated phylogenetic tree under the multispecies coalescent (MSC) model with SNAPP (Bryant et al., 2012), using its implementation in BEAST2 v.2.7.3 (Bouckaert et al., 2019) and the strict molecular clock model, following Stange et al. (2018). We generated the input file for SNAPP using *snapp_prep.rb* (https://github.com/mmatschiner/snapp_prep), applying a constraint on the

Downloaded from https://academic.oup.com/evolut/article/80/6/1311/8660089 by guest on 08 June 2026

divergence between *P. flavipunctatus* and the *P. rupestris* species complex with a lognormal prior distribution centered at 20.82 mya with a standard deviation of 0.08, based on the mean and the 95% highest posterior density (HPD) interval estimated by Burriel-Carranza et al. (2025b). Due to the high computational demand of SNAPP, we reduced the number of SNPs of the strictly filtered dataset from 2,098,690 to 10,000 randomly chosen SNPs, and simultaneously removed sites without genotype information for one or more species, as well as tri-allelic sites and tetra-allelic sites. We performed three replicate SNAPP runs, each with a length of 500,000 generations, sampling every 50 generations. We checked for convergence and stationary of the resulting combined Markov Chain Monte Carlo (MCMC) simulations in Tracer v.1.7.1 (Rambaut et al., 2018).

### Introgression analyses

To investigate the presence of introgression within the *P. rupestris* species complex, we calculated both Patterson's *D*-statistic and f4-ratio using Dsuite (Malinsky et al., 2021) with both permissive and strict datasets. The *D*-statistic quantifies imbalance in the sharing of ancestral and derived alleles among two sister lineages (P1 and P2), a third lineage (P3) diverged from their common ancestor, and an ancestral fourth lineage (P4). Individuals were assigned to species and genetically identified lineages (sensu Burriel-Carranza et al., 2025a), with *P. flavipunctatus* as the ancestral taxon, and the SNAPP genomic tree used as the underlying topology. The *D*-statistic and f4-ratio were calculated for all possible lineage trios and visualized in a heatmap.

Since the *D*-statistic can produce misleading signals when lineages have different evolutionary rates, we also ran tree-based introgression tests that have been shown to be reliable under these conditions (Koppetsch et al., 2024): $D_{\text{tree}}$, a test equivalent to *D*-statistic but based on frequencies of alternative rooted tree topologies for a given species trio (Ronco et al., 2021), and Species Networks applying Quartets (SNaQ), a maximum-likelihood inference method of phylogenetic networks under the MSC model with hybridization (Solís-Lemus & Ané, 2016). As input for these two tests, local trees sampled across the genome were generated as follows: contigs with <10 SNPs were removed using BCFtools v.1.15 (Li, 2011), and the remaining variants were phased with beagle v.5.4 (Browning & Browning, 2007). Genotypes previously missing or masked were re-masked after phasing (Ronco et al., 2021). Alignments of 5,000 bp were prepared, selecting one individual per lineage with the least missingness. Alignment blocks were extracted using *extract_blocks.rb* (https://raw.githubusercontent.com/mmatschiner/tutorials/refs/heads/master/analysis_of_introgression_with_chromosome_length_alignments/src/extract_blocks.rb) and filtered to exclude blocks with <25 parsimony-informative sites or >10 hemiplasies. Maximum-likelihood phylogenies were inferred using IQ-TREE v.2.2.2 (Minh et al., 2020), specifying *P. flavipunctatus* as outgroup. Uninformative trees with internal branches <0.001 substitutions per site were removed (Ronco et al., 2021), and the remaining trees were concatenated. $D_{\text{tree}}$ was run using *analyze_tree_asymmetry.rb* (Ronco et al., 2021), with counts of alternative rooted tree topologies tested for introgression significance via a one-sided binomial test. The same tree set was used as an input for SNaQ (Solís-Lemus & Ané, 2016), testing up to two reticulation events by quantifying concordance factors for unrooted species quartets and calculating likelihoods under the MSC with hybridization.

### Demographic history analyses

To infer the demographic history of the *P. rupestris* species complex, we used the pairwise sequential Markovian coalescent (PSMC) software (https://github.com/lh3/psmc). Heterozygous positions were identified from BAM files using SAMtools v.1.13 (Li et al., 2009), excluding samples with mapping or base quality <30. A generation time of 1 year was assumed for species of the *P. rupestris* complex (Ackermann, 2018), and the mutation rate was set to the mean squamate mutation rate ($1.75 \times 10^{-9}$ per site per year; Gemmell et al. (2020)). To evaluate variability in $N_e$ estimates, 15 bootstrap replicates were conducted per individual, and results were plotted per lineage and species using gnuplot v.5.4.2. We also calculated $\pi$ using pixy (Korunes & Samuk, 2021) to estimate $N_e$ under a constant population size assumption. Variants called with GATK (see above) were hard-filtered using GATK's "VariantFiltration" (GATK v.4.4; McKenna et al., 2010) for contigs >10 Mbp, excluding variants with strand bias >60 or strand odds ratio >3. Additional quality filters were mapping quality <40, mapping quality rank sum <−12.5, quality by depth <2, and read position rank sum <−8.0. Variants were further filtered with BCFtools v.1.15.1 (Li, 2011) to exclude depth <3, genotype quality <20, or reference genotype quality <20, retaining only high-confidence genotypes. Multiallelic sites and indels were removed. $\pi$ was then calculated in 100,000 bp windows for all contigs, and mean $\pi$ was inferred per genetic lineage.

## Results

### Phenotypic differentiation

Linear morphometric analyses of 83 individuals showed a broad overlap in body shape morphospace across the *P. rupestris* species complex (excluding the single individual of *P. assareen*) (Figure 2). The pairwise Procrustes distance comparisons based on the principal components of the PCA (explaining more than 50% of all shape variance) revealed no significant shape differences between *P. feulneri* and either *P. omanensis* or *P. rupestris* s.strc. In contrast, significant differences were found between *P. ali* and *P. feulneri*, *P. omanensis*, and *P. rupestris* s.strc. ($p = 0.001–0.006$), as well as between *P. omanensis* and *P. rupestris* s.strc. ($p = 0.023$) (Table S4). However, variance analyses indicated no significant differences in phenotypic dispersion among all the four species ($p > 0.05$) (Table S4). Procrustes ANOVA based on genetic lineage identity revealed significant variation in body shape ($p = 0.001$, $Z = 5.06$) (Tables S5 and S6). Also, pairwise Procrustes distance comparisons indicated that some lineages exhibited significant differences in body shape. Particularly, lineage BFD4 of *P. ali* showed the strongest divergence from all the other lineages ($p = 0.001–0.051$). However, some lineages, such as BFD11 and BFD6, displayed minimal differentiation from each other ($p > 0.1$). No significant differences in body shape were found among geographic regions ($p = 0.367$) (Figure S2). Also, phenotypic differences in body shape variation across elevations were not statistically significant ($p = 0.838$) (Figure S3).

Downloaded from https://academic.oup.com/evolut/article/80/6/1311/8660089 by guest on 08 June 2026

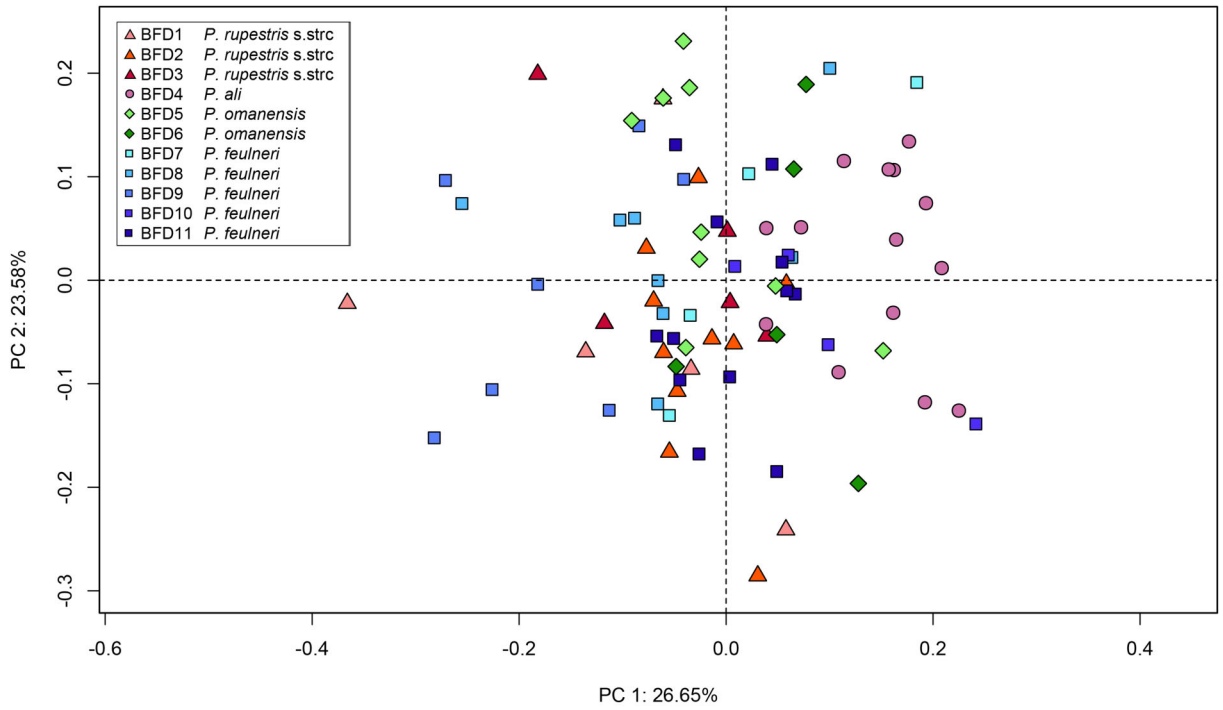



**Figure 2.** Reconstructed morphospace based on linear measurements of the different species (symbols) and genetic lineages (colors) across the *Pristurus rupestris* species complex. The first two principal components of the PCA explain more than 50% of all shape variance. The morphospace was constructed based on nine independent linear measurements of 84 *Pristurus* specimens corrected for the effect of body size (see the "Materials and Methods" section and Table S1). Neither species nor genetic lineages are well-separated in morphospace.

Geometric morphometrics based on 3D landmarks capturing head shape across the same 83 individuals of the *P. rupestris* species complex showed a strong overlap in morphospace among species (Figure 3). Procrustes ANOVA revealed no significant overall differences in head shape among *P. ali*, *P. feulneri*, *P. omanensis*, and *P. rupestris* s.strc. ($p = 0.314$) (Table S7). Pairwise Procrustes distance comparisons identified some degree of interspecific differentiation in head shape, though none of these differences were statistically significant ($p > 0.05$) after accounting for multiple comparisons. Variation in head shape was not significantly different across species ($p = 0.515$–$0.932$), with the lowest observed variance in *P. ali* (0.00315) and the highest in *P. rupestris* s.strc (0.00353) (all not significant; $p > 0.05$) (Table S7). Among the genetic lineages, the Procrustes ANOVA revealed significant variation in head shape ($p = 0.011$) (Tables S8 and S9). Pairwise comparisons highlighted high similarity in head shape, with 44 of 55 comparisons (80%) yielding nonsignificant differences ($p > 0.05$). Only 11 comparisons (20%) showed significant differentiation. Notably, lineages BFD8 ($p = 0.003$–$0.030$) and BFD11 ($p = 0.003$–$0.045$) of *P. feulneri* exhibited some distinctness in head shape relative to the other lineages. Head shape did not differ significantly among geographic regions ($p = 0.298$) (Figure S4). Variance was slightly lower at high elevations (0.0032) than at low elevations (0.0037), but this difference was not significant ($p = 0.286$) (Figure S5). Trajectory analysis revealed that *P. ali* exhibited a significantly greater path distance than *P. feulneri* ($p = 0.011$), and indicated cranial shape convergence at high elevations ($p = 0.075$) (Figure S6). Phylomorphospace patterns of comparisons between *P. ali*, *P. feulneri*, and *P. rupestris* s. strc. showed no clear disparity differences but strong clade overlap (Figure S7).

## Genome assembly

Using PacBio HiFi sequencing, we obtained the first de novo reference genome assembly for the genus *Pristurus*. The final assembly for *P. rupestris* s. strc. spans 2.3 Gbp, with a scaffold N50 length of 7.5 Mbp, and a longest scaffold with a length of 57 Mbp (Figure S8). The BUSCO analysis revealed a 98.5% completeness of metazoan ortholog groups, and a GC content of 44.8% (Figure S8). The BlobToolKit test showed that only 3.9 Mbp (0.17%) of the final assembly were assigned to non-Chordata or did not match to a metazoan phylum at all (Figure S9). Diploidy was confirmed with the k-mer analysis using SmudgePlot, indicating 81% of all heterozygous k-mer pairs as diploid and only about 19% as triploid or tetraploid (Figure S10 and S11). The final genome assembly was stored and is available on NCBI under the BioProject PRJNA1444514.

## Phylogenomic reconstruction

To investigate the evolutionary relationships within the *P. rupestris* species complex, we inferred a time-calibrated phylogenetic tree under the MSC model (Figure 4). We recovered a monophyletic clade formed by *P. ali*, *P. assareen*, *P. feulneri*, *P. omanensis*, and *P. rupestris* s. strc. The topology within this clade is congruent with a recent phylogeny based on ddRAD data (Burriel-Carranza et al., 2025a), as well as previous phylogenetic analyses of the complex (Badiane et al., 2014; Garcia-Porta et al., 2017). Interspecific divergence times within the *P. rupestris* species complex were found to be even older than those reported recently by Burriel-Carranza et al. (2025a), ranging from about 16.5 to 6 million years ago (Ma), and more similar to the estimates of Garcia-Porta et al. (2017). We estimated the time

Downloaded from https://academic.oup.com/evolut/article/80/6/1311/8660089 by guest on 08 June 2026

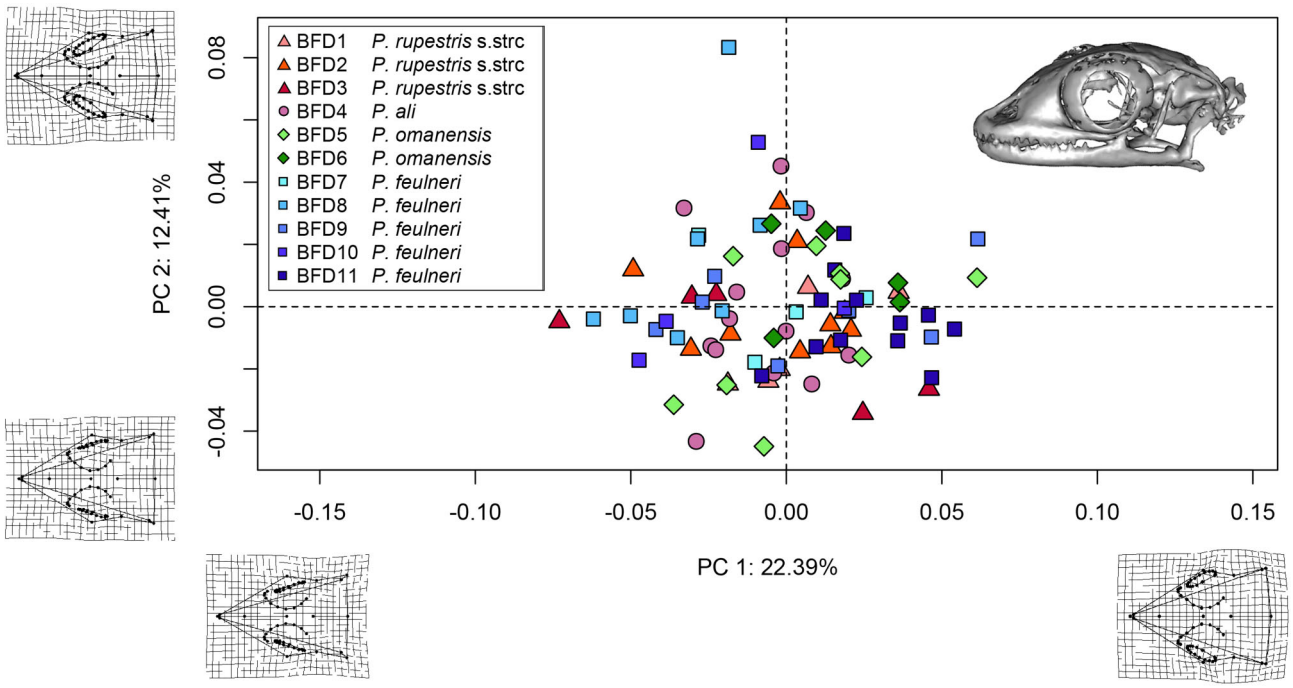



**Figure 3.** Reconstructed morphospace based on landmark-based 3D shape analyses of head shape for the different species (symbols) and genetic lineages (colors) across the *Pristurus rupestris* species complex represented by the first two principal components of the PCA (explaining more than 34% of all shape variance). The morphospace was constructed based on 67 landmarks and semilandmarks of 84 *Pristurus* specimens and corrected for the effect of body size (see the "Materials and Methods" section). Both species and genetic lineages show a great overlap across their morphospace. Extreme head shape phenotypes along the first two principal components are given below the corresponding coordinate axes. A typical three-dimensional skull model of *Pristurus rupestris* (lateral view; see Figure S1 for landmarking scheme) is shown in the top-right panel of the PCA plot.

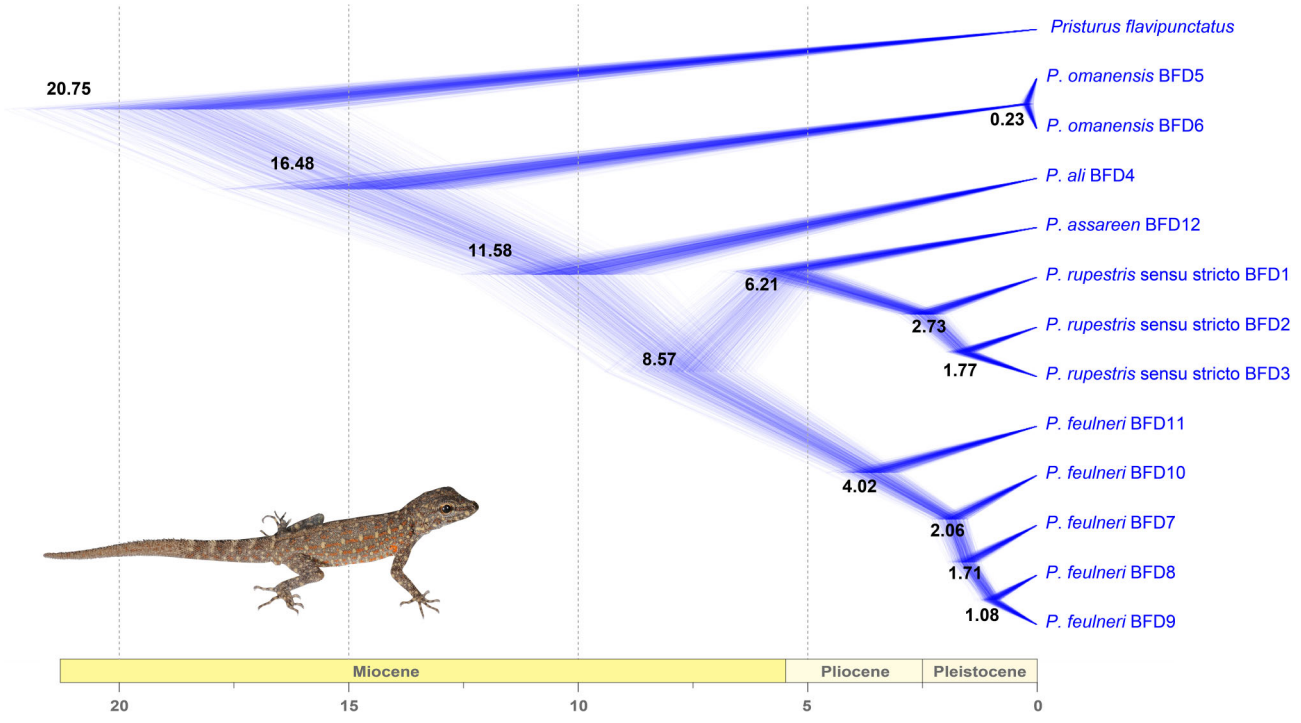



**Figure 4.** Robust genomic phylogeny of the entire radiation of the *Pristurus rupestris* species complex. Time-calibrated tree inferred under the multispecies coalescent model for the genetic lineages and species of the *Pristurus rupestris* species complex defined in Burriel-Carranza et al. 2025b. Two *P. flavipunctatus* specimens are used as outgroup. Mean divergence-time estimates are shown at each node. All nodes are supported by a posterior probability of 1. The strict dataset comprising 2,098,690 SNPs was used for the phylogenomic reconstruction (see the "Material and Methods" section ). The geological time scale is color coded according to the International Chronostratigraphic Chart. Inset picture shows a specimen of *P. feulneri*.

Downloaded from https://academic.oup.com/evolut/article/80/6/1311/8660089 by guest on 08 June 2026

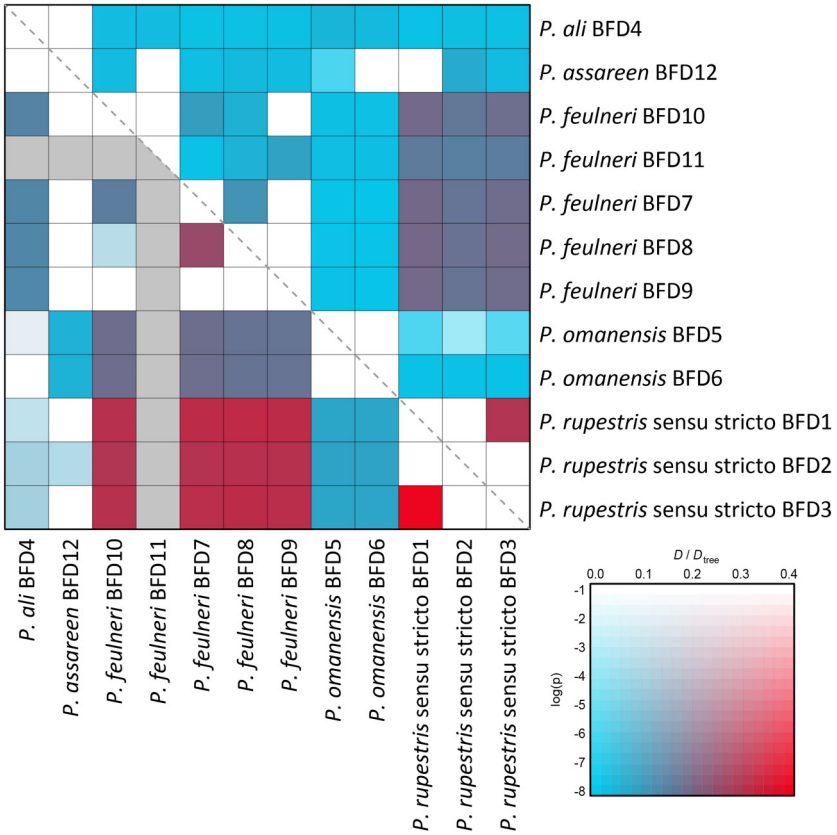



**Figure 5.** Signals of introgression among the genetic lineages of the *Pristurus rupestris* species complex. Upper matrix: Patterson's *D*-statistic with corresponding *p*-values for all possible combinations of trios of the 12 genetic *Pristurus* lineages defined. Lower matrix: Signals of introgression among 11 lineages of the *Pristurus rupestris* species complex indicated by the $D_{tree}$-statistic. This test is equivalent to the *D*-statistic, but based on frequencies of alternative rooted tree topologies for a given species trio. The heat map is showing the $D_{tree}$-statistic with corresponding *p*-values for all possible combinations of trios of the genetic *Pristurus* lineages defined. Lineage BDF 11 of *P. feulneri* (in gray) was excluded due to a high proportion of missing data. The two different approaches uncovered genetic exchange both among and across *P. feulneri* and *P. rupestris* s. str.

of divergence between *P. flavipunctatus* and the *P. rupestris* species complex at 20.75 Ma (95% HPD: 17.73–24.07 Ma). Within the latter radiation, *P. omanensis* was found to have split 16.48 Ma (95% HPD: 13.83–19.07 Ma) from the other representatives of the species complex. Then *P. ali* diverged 11.58 Ma (95% HPD: 9.81–13.52 Ma) from a monophyletic group encompassing two clades that diverged 8.57 Ma (95% HPD: 7.16–9.91 Ma): one clade with *P. assareen* and *P. rupestris* s. strc., and another clade with *P. feulneri*. Around 6.21 Ma (95% HPD: 5.25–7.24 Ma), *P. assareen* separated from *P. rupestris* s. strc. Divergence times of the intraspecific genetic lineages defined by Burriel-Carranza et al. (2025b) ranged from 4.02 Ma (95% HPD: 3.37–4.7 Ma) within *P. feulneri* to 0.23 Ma (95% HPD: 0.11–0.36 Ma) within *P. omanensis*.

## Introgression analyses

Using the permissive dataset of 86,977,236 SNPs, we tested for the presence of introgression between the different species and genetic lineages of the *P. rupestris* species complex. By calculating the commonly used *D*-statistic and f4-ratio, as well as applying the two tree-based introgression tests, $D_{tree}$ and SNaQ, we found both intra- and interspecific signals of genetic exchange. The *D*-statistic significantly supported introgression within *P. rupestris* s. strc. between the genetic lineages BDF1 and BDF3 with $D = 0.256$ ($p = 2.3 \times 10^{-16}$) (Figure 5). Allele sharing between these two clades was also supported by the corresponding f4-ratio (0.188) (Figure S12). In addition, the *D*-statistic revealed positive signals of interspecific genetic exchange between the five genetic lineages of *P. feulneri* and three lineages of *P. rupestris* s. strc. with significant *D*-values ranging from 0.156 to 0.192 (Figure 5). The results of the $D_{tree}$-test confirmed the introgression events detected by the *D*-statistic, but revealed an additional significant signal of intraspecific genetic exchange ($D = 0.113$) within *P. feulneri* between the lineages BFD7 and BFD8 (Figure 5). The species-level topology of the backbone tree recovered by SNaQ was concordant with the phylogenomic reconstruction using SNAPP, with only minor differences for the internal positions of some genetic lineages within *P. feulneri* and *P. rupestris* s. strc. (Figure 6). Given a maximum number of two reticulation events, SNaQ supported a reticulation involving the common ancestor of *P. feulneri* and *P. feulneri* BFD8, suggesting genetic exchange within *P. feulneri* between a presumably unsampled ghost lineage and *P. feulneri* BFD8 (Figure 6). Another reticulation event was found between *P. rupestris* s. strc. lineage BDF1 and the ancestor of *P. feulneri* (Figure 6).

## Demographic histories

The demographic history of each representative of the *P. rupestris* species complex was inferred with PSMC analy-

Downloaded from https://academic.oup.com/evolut/article/80/6/1311/8660089 by guest on 08 June 2026

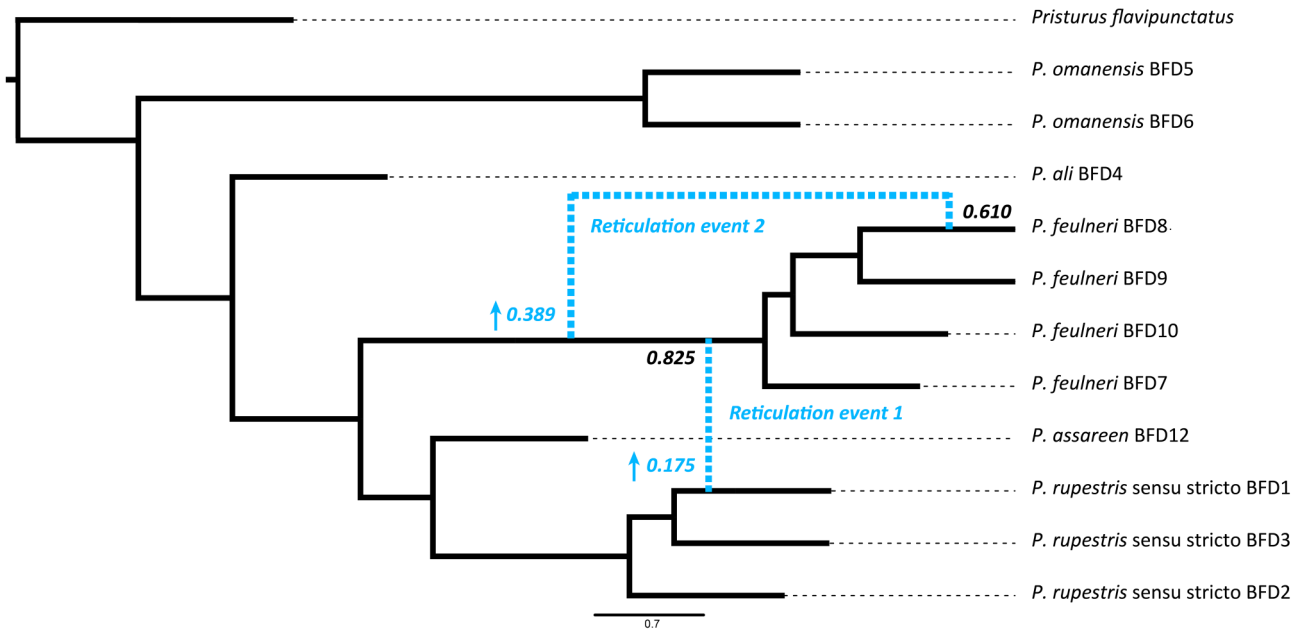



**Figure 6.** Phylogenetic network indicating occurrence and direction of genetic exchange among the *Pristurus rupestris* species complex. Topology and reticulation events were uncovered by Species Networks applying Quartets (SNaQ), a maximum-likelihood inference method of phylogenetic networks based on the multispecies coalescent model with hybridization. Reticulation events are represented by blue dotted lines, with numbers indicating the proportion of alleles inherited from each involved lineage (arrow indicating direction of genetic exchange from donor lineage to recipient lineage).

ses, which revealed strong interspecific differences in past population dynamics (Figure 7), but for some taxa, comparable changes in $N_e$ among intraspecific lineages (Figures S13–S15). While *P. assareen* and *P. omanensis* did not show rapid changes in past population size, opposite patterns were found for the other species of the radiation. Effective population sizes for the three genetic lineages of *P. rupestris* s. strc. fluctuated between 1 million and 100,000 years ago, with particular sharp increases and declines in $N_e$ for lineage BDF2, while all lineages showed a population decline about 30,000 years ago. Between 1 million and 300,000 years ago, both *P. ali* and *P. feulneri* showed a moderate decline in $N_e$. For *P. ali*, increasing levels in population size were found about 100,000 years ago, followed by a slight decline about 30,000 years ago, and a moderate to rapid increase about 20,000 years ago. Some lineages of *P. feulneri* showed population growth about 100,000 years ago, and fluctuations and a more rapid increase toward the presence, about 20,000 years ago. Effective population sizes calculated with pixy under the assumption of a constant population size complemented the results of the PSMC analysis (Figure 7). Using pixy, the highest $N_e$ was found for *P. ali* with about 1.3 million individuals. For the lineages of *P. rupestris* s. strc., $N_e$ ranged from about 640,000 to 1 million individuals, for *P. feulneri* from about 520,000 to 1 million individuals, for *P. omanensis* from 635,000 to 690,000 individuals, and for *P. assareen* about 680,000 individuals (Figure 7).

## Discussion

Recent years have seen an exponential growth in the availability of reference genome data for vertebrates (Rhie et al., 2021). However, the proportion of high-quality genome assemblies relative to described species diversity remains substantially lower in squamates and amphibians than in mammals and birds. Among squamates (Card et al., 2023; Gable et al., 2023; Pinto et al., 2023), Gekkota are particularly underrepresented, with approximately 30 available reference genomes despite encompassing 2,466 recognized species (Uetz et al., 2025). The family Sphaerodactylidae alone comprises 239 species, yet genomic resources remain scarce: Apart from the two New World species *Sphaerodactylus glaucus* Cope, 1866 and *S. townsendi* Grant, 1931, this study provides only the third reference genome for an Old World sphaerodactylid gecko, *P. rupestris* s. strc., alongside *Euleptes europaea* (Gené, 1839) and *Teratoscincus roborowskii* Bedriaga, 1906 (Feiner et al., 2025).

In the present study, we integrated geometric morphometric analyses with phylogenomic reconstructions across deeply divergent lineages within the extraordinary radiation of *Pristurus* geckos in the southeastern Arabian Hajar Mountains, accounting for intraspecific genetic structure. We investigated phenotypic differentiation and its evolutionary significance for the five species of the *P. rupestris* species complex—*P. ali*, *P. assareen*, *P. feulneri*, *P. omanensis*, and *P. rupestris* s. strc. We present whole-genome data for all genetic lineages previously identified within this radiation (Burriel-Carranza et al., 2025a; Garcia-Porta et al., 2017) and generated a reference genome for a topotypical specimen of *P. rupestris* s. strc. Despite a lack of clear phenotypic differences among species, our findings reveal deep divergences within this radiation, dating back more than 16 Ma and extending the age estimates recently reported by Burriel-Carranza et al. (2025b). Moreover, we found evidence of genetic exchange both within and across species, along with striking interspecific differences in demographic histories. Our study underscores the prevalence of strong phenotypic crypticity despite deep phylogenetic divergence, highlighting the complex evolutionary history of this radiation of *Pristurus* geckos.

Downloaded from https://academic.oup.com/evolut/article/80/6/1311/8660089 by guest on 08 June 2026

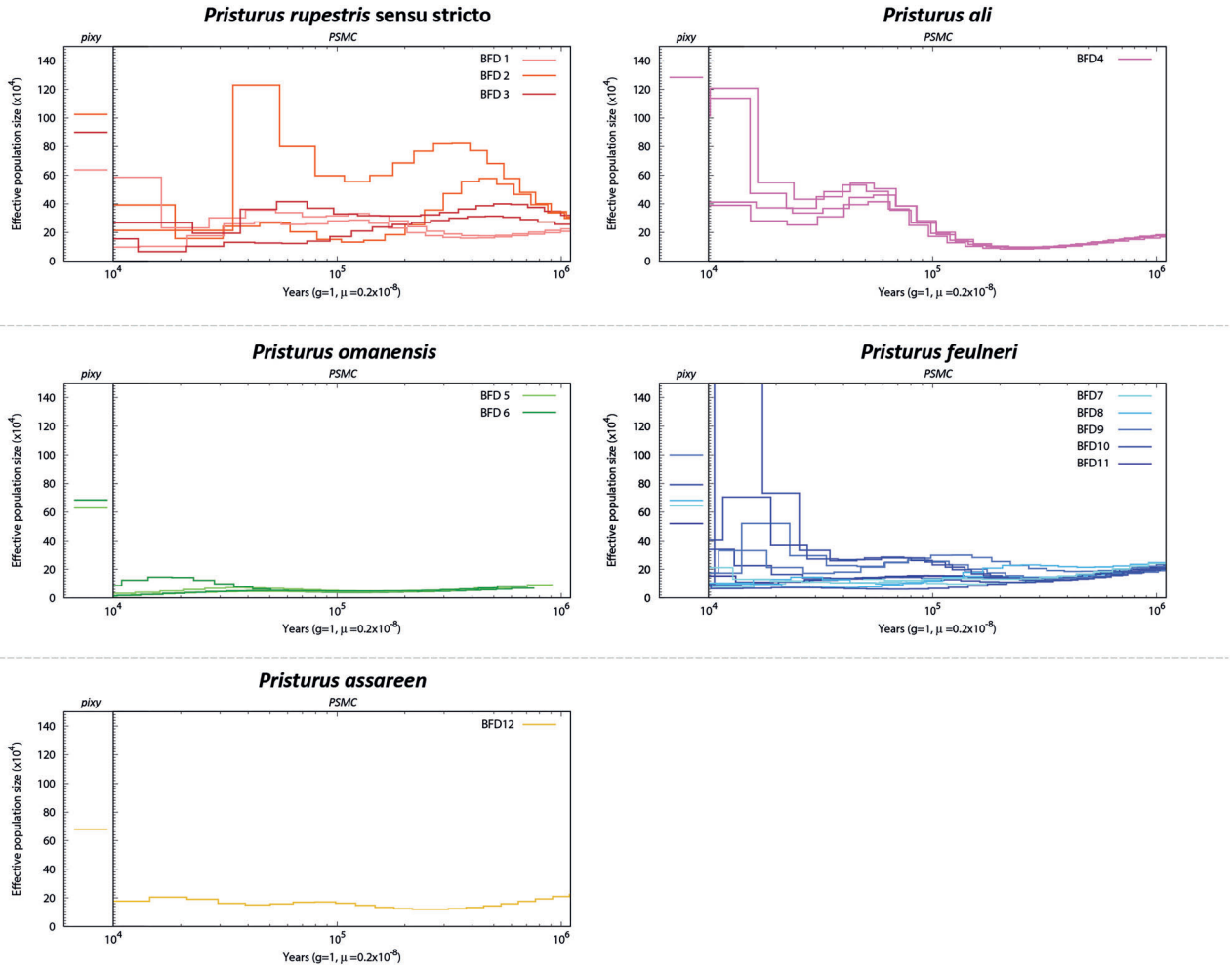



**Figure 7.** Demographic history analysis and effective population size of the *Pristurus rupestris* species complex. Demographic histories were reconstructed with pairwise sequential Markovian coalescent (PSMC) for all species and genomic lineages of the *P. rupestris* species complex in the Hajar Mountains. A generation time of one year and a substitution rate of $1.75 \times 10^{-9}$ per site per year were assumed. Estimates of effective population size ($N_e$) shown on the left of each PSMC plot were calculated with pixy under the assumption of a constant population size over time.

Our morphometric analyses of both external phenotypic traits and internal cranial osteology highlight a substantial overlap in both body shape and head shape within the *P. rupestris* species complex (Figures 2 and 3). Previous studies have already suggested a high degree of crypsis for this *Pristurus* radiation (Badiane et al., 2014; Garcia-Porta et al., 2017), as extensive morphological variability within and between species obscures clear external diagnostic characters (Burriel-Carranza et al., 2025a). Moreover, the broad overlap in head shape indicates that no clear differentiation in skull morphology exists among species, further supporting interspecific similarities in various ecological and functional traits associated with cranial morphology, e.g., bite force or feeding ecology (Herrel et al., 2001; Kaliontzopoulou et al., 2012). Additionally, the existence of two ecologically distinct phenotypes—a robust high-elevation morphotype and a slender low-elevation morphotype—could not be clearly assigned to specific species or genetic lineages. Instead, our findings suggest that this pattern may be driven by the apparent convergence in head shape among individuals from high elevations as suggested by Garcia-Porta et al. (2017) (Figure S6), reflecting the presence of ecological constraints specific to arid high-altitude mountains. While intraspecific morphological differentiation was found for specific lineages, for example, among lineages of *P. feulneri*, no significant differences in morphological disparity were detected at the interspecific level. Further insights into patterns of intraspecific variation would require a more comprehensive and balanced sampling across lineages and environmental categories. So far, the possible causes of notable phenotypic similarity in the *P. rupestris* species complex remain unclear. In other small-sized geckos, miniaturization has been linked to reduced skull variation and a high degree of morphospace overlap, likely due to strong structural constraints on skull architecture (Daza et al., 2008; Rieppel, 1984). This pattern has been particularly well-documented in the nonadaptive radiation of miniaturized day geckos of the genus *Lygodactylus* (Lobón-Rovira et al., 2024), where evolutionary constraints limit cranial diversification despite species richness. Such constraints may similarly contribute to the observed overlap in skull morphology within the miniaturized species of the *P. rupestris* complex, potentially restricting the extent of morphological divergence.

Downloaded from https://academic.oup.com/evolut/article/80/6/1311/8660089 by guest on 08 June 2026

Morphological stasis in the *P. rupestris* species complex may have been driven by niche conservatism and a strong reliance on rocky microhabitats in arid environments (Arnold, 1993, 2009). These factors could have shaped adaptive optima that are maintained by stabilizing selection, preventing significant morphological divergence despite deep evolutionary splits. Similar patterns have been observed in other phenotypically cryptic yet phylogenetically divergent squamate species (Guarnizo et al., 2016; Marín et al., 2018), where strong selective pressures constrain morphological evolution. Smith et al. (2011) demonstrated that species in a cryptic agamid lizard complex (*Diporiphora*) exhibit a history of constrained phenotypic evolution, with lineages showing a tendency to revert to an intermediate morphological state over time. While our trajectory analysis of head shape variation (Figure S6) indicates that cranial shape evolved independently at high elevations in a lineage-specific manner for *P. rupestris* and *P. ali*, *P. feulneri* exhibits little to no morphological change with elevation. This suggests that in extreme high-elevation environments, stabilizing selection may help maintain morphological similarity despite ongoing genetic divergence. This pattern of constrained phenotypic evolution aligns with broader evidence that environmental constraints can shape and maintain morphological stasis in squamates across evolutionary timescales, particularly in harsh habitats. Such cases have been documented for other geckos from harsh arid environments, e.g., cryptic *Diplodactylus* species, which also exhibit striking phenotypic similarities despite deep phylogenetic splits (McDonald et al., 2024), further supporting the role of ecological pressures in limiting morphological divergence. Overall, while ecological pressures may drive convergence in certain lineages of the *P. rupestris* species complex, the pervasive morphological similarity across the radiation likely also reflects developmental or structural constraints that limit diversification, reinforcing the combined roles of intrinsic and extrinsic factors in shaping phenotypic stasis.

Characteristic for *Pristurus* geckos is their unique behavior and intraspecific communication by body compression, limb and throat extension, and caudal signaling, the latter involving tail waving and curling (Ackermann, 2018; Ackermann & Zwanzig, 2018; Arnold, 1993, 2009). The strong overlap in head shape (Figure 3) and overall similarity in body morphometrics (Figure 2) shown by our phenotypic analyses confirm the lack of clear external morphological diagnostic traits allowing to distinguish taxa within the *P. rupestris* species complex. However, the absence of distinct visual traits does not preclude the possibility that these species exhibit behavioral differences facilitating species-specific recognition. Differences in communication signals, territorial displays, and mate choice could play a crucial role in maintaining species boundaries despite morphological similarity.

Phylogenomic reconstruction and divergence time estimates revealed deep evolutionary splits within the *Pristurus* radiation in the Hajar Mountains (Figure 4). Interspecific divergences within the *P. rupestris* species complex range from approximately 16.5 to 6 million years ago, substantially older than estimates reported recently for the same group by Burriel-Carranza et al. (2025a) and more comparable to estimates from Garcia-Porta et al. (2017). These deep Miocene splits indicate that recent divergence cannot explain the pronounced phenotypic similarity observed among lineages. This stands in contrast to examples of other species-rich yet phenotypically constrained groups of geckos, such as the recently diverged nonadaptive radiation of the New Caledonian genus *Bavayia*, occurring as recently as the Pliocene (Bauer et al., 2022). The relatively old age of the *P. rupestris* species complex, combined with its pronounced phenotypic similarity, underscores its unique evolutionary history among geckos and reinforces the Hajar Mountains as a long-term biodiversity reservoir. These deep divergences demonstrate that morphological stasis can be maintained over tens of millions of years, making this one of the oldest known cases of cryptic diversification in an Arabian reptile hotspot (Burriel-Carranza et al., 2025b). Remarkably, the intrageneric splits within this radiation are older than those in many other gecko groups at comparable taxonomic levels, further highlighting the extraordinary evolutionary persistence of morphologically similar lineages in this system. For instance, whereas most intrageneric and generic diversity in various diplodactylid geckos has accumulated relatively recently (Oliver & Sanders, 2009; Skipwith et al., 2016), the deep splits between major clades at higher taxonomic levels in their phylogeny are more comparable in age to those observed at species level within the *Pristurus* radiation.

Introgression analyses (Figure 5) revealed that hybridization is confined to specific lineage pairs, and so it cannot explain the widespread phenotypic similarities across the *P. rupestris* species complex. The restricted pattern of introgression detected here most likely reflects historical episodes of secondary contact rather than ongoing gene flow among extant populations, contrasting with patterns reported for other geckos in the Hajar Mountains, e.g., *Trachydactylus hajarensis* (Burriel-Carranza et al. 2023a). Such ancient admixture events could represent past range shifts and climatic oscillations that may have facilitated transient contact between now-divergent lineages, leaving localized genomic signatures of introgression. Given the deep divergences, prezygotic barriers, such as Muller–Dobzhansky incompatibilities, may prevent ongoing genetic exchange despite sympatric or even syntopic occurrences of representatives of the *P. rupestris* species complex, as observed for *P. assareen* and *P. rupestris* s. str. (Burriel-Carranza et al., 2026). Therefore, rather than being the result of ongoing gene flow producing intermediate phenotypes, these morphological similarities are more likely driven by shared environmental pressures and stabilizing selection that limit divergence in skull morphology, despite the deep genetic splits. In addition, pronounced fluctuations in population dynamics (Figure 7) underscore the distinct demographic histories of the five species within the *Pristurus* radiation. The observation of unexpectedly high estimates of effective population sizes in range-restricted species, such as *P. ali*, suggests complex historical shifts in population densities or distribution ranges. These patterns may reflect past environmental fluctuations, habitat fragmentation, or varying levels of connectivity between populations over time. Still, unlike other species-rich gecko diversifications, such as *Cyrtodactylus*—the third most speciose vertebrate genus (Grismer et al., 2021a, 2021b)—our morphometric analyses revealed that species of the *P. rupestris* complex do not exhibit a strong correlation between microendemism and ecomorphological

Downloaded from https://academic.oup.com/evolut/article/80/6/1311/8660089 by guest on 08 June 2026

diversification. This is despite the fact that some species, like *P. ali* or *P. assareen*, are highly microendemic and have very restricted distributions, with the latter restricted to Wadi As Sareen Nature Reserve (Burriel-Carranza et al., 2026), ranking among the Arabian reptiles with the most restricted ranges (Burriel-Carranza et al., 2025a; Meiri et al., 2018).

Overall, our results highlight the *P. rupestris* species complex in the Hajar Mountains as a remarkable system for studying evolutionary history and adaptations in squamates, offering a rare combination of deep phylogenetic divergence and strong phenotypic similarity. The contrast between the substantial genetic differentiation among species and their overlapping external morphology underscores the complexity of evolutionary processes shaping this radiation. In light of Struck et al.'s (2018) framework, our data suggest that the crypticity in the *Pristurus* radiation in the Hajar Mountains is driven by phenotypic stasis in the face of ecological limitations, rather than recent divergence, given the persistent morphological similarity despite significant genetic differentiation. Moreover, we found indications of an additional level of cryptic differentiation within the *P. rupestris* species complex, given that the high-elevation type evolved independently from the low-elevation one in different species. With the addition of extensive whole-genome data and a new de novo reference genome for an Old World sphaerodactylid gecko, this system provides an unparalleled opportunity to investigate the interplay of selection, phenotypic stasis, and gene flow in shaping diversification. Future studies integrating transcriptomic data could reveal whether specific genes or regulatory elements contribute to maintaining morphological similarity despite evolutionary divergence. Additionally, behavioral and ecological studies are needed to unravel the mechanisms that maintain species boundaries in the absence of clear morphological differentiation, ultimately providing deeper insights into how squamates adapt and diversify in extreme arid environments.

## Supplementary material

Supplementary material is available online at *Evolution*.

## Data availability

The reference genome assembly of *Pristurus rupestris* sensu stricto, as well as whole genome sequencing Illumina raw data for 30 specimens comprising the *Pristurus rupestris* species complex (*Pristurus ali*, *P. assareen*, *P. feulneri*, *P. omanensis*, and *P. rupestris*) and *P. flavipunctatus* are available on NCBI under the BioProject PRJNA1444514. Code for all morphological and phylogenomic analyses is available on https://github.com/thorekop/Pristurus_DiversificationDynamics. All supplementary figures and metadata are provided in Supplementary Material, or are accessible through the Dryad repository (DOI: 10.5061/dryad.jq2bvq8qx).

## Author contributions

Conceptualization: T.K., D.C.A., S.C., and M.M. Supervision: D.C.A., S.C., A.J., and M.M. Project Administration: T.K. Investigation: T.K. Formal Analysis: T.K. Methodology: T.K. Data Curation: T.K., B.B.C., E.G., X.Z.L. Resources: T.K., B.W., S.C., and M.M. Visualization: T.K., B.B.C. Writing—Original Draft Preparation: T.K. Writing—Review & Editing: T.K., B.B.C., E.G., A.J., D.C.A., S.C., and M.M.

## Funding

This work was funded by grant PID2021-128901NB-I00MCIN/AEI/10.13039/501100011033, by the European Regional Development Fund—"A way of making Europe," and by the Natural History Museum, University of Oslo.

## Conflict of interest

The authors declare no conflict of interest.

## Acknowledgments

We would like to thank the past and present members of the Ministry of Environment and Climate Affairs, MECA, Oman, now the Environment Authority Oman, and especially to Ali Al Kiyumi, Suleiman Nasser Al Akhzami, Thuraya Al Sariri, Saleh Al Saadi, Ahmed Said Al Shukaili, Ali Alghafri, Sultan Khalifa, Hamed Al Farqani, Salim Bait Bilal, Iman Sulaiman Alzari, Aziza Saud Al Adhoobi, Mohammed Al Shariani, Zeyana, Salim Al Omairi and Abdullah bin Ali Al Amri, Chairman of the Environment Authority. We are also very grateful to present and past collaborators, including Edwin Nicholas Arnold, Michael D. Robinson, Andrew Gardner, Josep Roca, Fèlix Amat, Philip de Pous, Margarita Metallinou, Joan Garcia-Porta, Raquel Vasconcelos, Roberto Sindaco, Gabriel Mochales-Riaño, Adrian Talavera, Sergi Tulloch, and Maria Estarellas for their help and support in the *Pristurus rupestris* project. We are thankful to Juliane Vehof for valuable help with microCT scanning of specimens, and Wolfgang Böhme and Ursula Bott for logistical support. We are grateful to Torsten H. Struck for his insights on the terminology of cryptic species and comments on an earlier version of the manuscript, as well as Kjetil L. Voje for help with statistical analysis. All computations were performed on resources provided by Sigma2—the National Infrastructure for High Performance Computing and Data Storage in Norway.

## References

Ackermann, T. (2018). Von Rollern und Wedlern: Zur Haltung und Vermehrung verschiedener *Pristurus* cf. *rupestris* im Terrarium. *SAURIA*, *40*, 27–48.

Ackermann, T., & Zwanzig, B.-M. (2018). *Pristurus minimus*—kleine Geckos mit großem Ego: Zur Haltung und Vermehrung im Terrarium. *SAURIA*, *40*, 1–12.

Adams, D. C., Berns, C. M., Kozak, K. H., & Wiens, J. J. (2009). Are rates of species diversification correlated with rates of morphological evolution? *Proceedings of the Royal Society B*, *276*, 2729–2738. https://doi.org/10.1098/rspb.2009.0543

Adams, D. C., Collyer, M., Kaliontzopoulou, A., & Sherratt, E. (2021). *Geomorph: Software for geometric morphometric analyses (R package version 4.0)*. Comprehensive R Archive Network.

Adams, D. C., Rohlf, F. J., & Slice, D. E. (2013). A field comes of age: Geometric morphometrics in the 21st century. *Hystrix, the Italian Journal of Mammalogy*, *24*, 7–14.

Agarwal, I., Bauer, A. M., Jackman, T. R., & Karanth, P. (2014). Cryptic species and Miocene diversification of Palaearctic naked-toed geckos (Squamata: Gekkonidae) in the Indian dry zone. *Zoologica Scripta*, *43*, 455–471. https://doi.org/10.1111/zsc.12062

Downloaded from https://academic.oup.com/evolut/article/80/6/1311/8660089 by guest on 08 June 2026

Arnold, E. N. (1993). Historical changes in the ecology and behaviour of semaphore geckos (*Pristurus*, Gekkonidae) and their relatives. *Journal of Zoology*, *229*, 353–384. https://doi.org/10.1111/j.1469-7998.1993.tb02642.x

Arnold, E. N. (2009). Relationships, evolution and biogeography of semaphore geckos, *Pristurus* (Squamata, Sphaerodactylidae) based on morphology. *Zootaxa*, *2060*, 1–21. https://doi.org/10.11646/zootaxa.2060.1.1

Badiane, A., Garcia-Porta, J., Červenka, J., Kratochvíl, L., Sindaco, R., Robinson, M. D., Morales, H., Mazuch, T., Price, T., Amat, F., Shobrak, M. Y., Wilms, T., Simó-Riudalbas, M., Ahmadzadeh, F., Papenfuss, T. J., Cluchier, A., Viglione, J., & Carranza, S. (2014). Phylogenetic relationships of semaphore geckos (Squamata: Sphaerodactylidae: *Pristurus*) with an assessment of the taxonomy of *Pristurus rupestris*. *Zootaxa*, *3835*, 33–58. https://doi.org/10.11646/zootaxa.3835.1.2

Baken, E. K., Collyer, M. L., Kaliontzopoulou, A., & Adams, D. C. (2021). Geomorph v4.0 and gmshiny: Enhanced analytics and a new graphical interface for a comprehensive morphometric experience. *Methods in Ecology and Evolution*, *12*, 2355–2363. https://doi.org/10.1111/2041-210X.13723

Barata, M., Carranza, S., & Harris, D. J. (2012). Extreme genetic diversity in the lizard *Atlantolacerta andreanskyi* (Werner, 1929): A montane cryptic species complex. *BMC Ecology and Evolution*, *12*, 167. https://doi.org/10.1186/1471-2148-12-167

Bauer, A. M., Sadlier, R. A., & Jackman, T. R. (2022). A revision of the genus *Bavayia* Roux, 1913 (Squamata: Gekkota: Diplodactylidae), a non-adaptive radiation of microendemic species. *Proceedings of the California Academy of Sciences*, *67*(Supplement I), 1–236.

Bickford, D., Lohman, D. J., Sodhi, N. S., Ng, P. K. L., Meier, R., Winker, K., Ingram, K. K., & Das, I. (2007). Cryptic species as a window on diversity and conservation. *Trends in Ecology & Evolution*, *22*(3), 148–155. https://doi.org/10.1016/j.tree.2006.11.004

Bookstein, F., Schäfer, K., Prossinger, H., Seidler, H., Fieder, M., Stringer, C., Weber, G. W., Arsuaga, J.-L., Slice, D. E., Rohlf, F. J., Recheis, W., Mariam, A. J., & Marcus, L. F. (1999). Comparing frontal cranial profiles in archaic and modern *Homo* by morphometric analysis. *The Anatomical Record*, *257*, 217–224. https://doi.org/10.1002/(SICI)1097-0185(19991215)257:6%3c217::AID-AR7%3e3.0.CO;2-W

Boratyn, G. M., Camacho, C., Cooper, P. S., Coulouris, G., Fong, A., Ma, N., Madden, T. L., Matten, W. T., McGinnis, S. D., Merezhuk, Y., Raytselis, Y., Sayers, E. W., Tao, T., Ye, J., & Zaretskaya, I. (2013). BLAST: A more efficient report with usability improvements. *Nucleic Acids Research*, *41*, W29–W33. https://doi.org/10.1093/nar/gkt282

Boratynski, Z., Brito, J. C., & Mappes, T. (2012). The origin of two cryptic species of African desert jerboas (Dipodidae: *Jaculus*). *Biological Journal of the Linnean Society*, *105*, 435–445. https://doi.org/10.1111/j.1095-8312.2011.01798.x

Bouckaert, R., Vaughan, T. G., Barido-Sottani, J., Duchêne, S., Fourment, M., Gavryushkina, A., Heled, J., Jones, G., Kühnert, D., De Maio, N., Matschiner, M., Mendes, F. K., Müller, N. F., Ogilvie, H. A., du Plessis, L., Popinga, A., Rambaut, A., Rasmussen, D., Siveroni, I., … Drummond, A. J. (2019). BEAST 2.5: An advanced software platform for Bayesian evolutionary analysis. *PLOS Computational Biology*, *15*, e1006650. https://doi.org/10.1371/journal.pcbi.1006650

Brandt, A., Brix, S., Held , C., & Kihara, T. C. (2014). Molecular differentiation in sympatry despite morphological stasis: Deep-sea *Atlantoserolis* Wägele, 1994 and *Glabroserolis* Menzies, 1962 from the south-west Atlantic (Crustacea: Isopoda: Serolidae). *Zoological Journal of the Linnean Society*, *172*, 318–359. https://doi.org/10.1111/zoj.12110

Brasier, M. J., Wiklund, H., Neal, L., Jeffreys, R., Linse, K., Ruhl, H., & Glover, A. G. (2016). DNA barcoding uncovers cryptic diversity in 50% of deep-sea Antarctic polychaetes. *Royal Society Open Science*, *3*, 160432. https://doi.org/10.1098/rsos.160432

Brito, J. C., Godinho, R., Martínez-Freiría, F., Pleguezuelos, J. M., Rebelo, H., Santos, X., Vale, C. G., Velo-Antón, G., Boratyński, Z., Carvalho, S. B., Ferreira, S., Gonçalves, D. V., Silva, T. L., Tarroso, P., Campos, J. C., Leite, J. V., Nogueira, J., Álvares, F., Sillero, N., … Carranza, S. (2014). Unravelling biodiversity, evolution and threats to conservation in the Sahara-Sahel. *Biological Reviews*, *89*, 215–231. https://doi.org/10.1111/brv.12049

Browning, S. R., & Browning, B. L. (2007). Rapid and accurate haplotype phasing and missing-data inference for whole-genome association studies by use of localized haplotype clustering. *The American Journal of Human Genetics*, *81*, 1084–1097. https://doi.org/10.1086/521987

Bryant, D., Bouckaert, R., Felsenstein, J., Rosenberg, N. A., & RoyChoudhury, A. (2012). Inferring species trees directly from biallelic genetic markers: Bypassing gene trees in a full coalescent analysis. *Molecular Biology and Evolution*, *29*, 1917–1932. https://doi.org/10.1093/molbev/mss086

Burriel-Carranza, B., Els, J., & Carranza, S. (2022). *Reptiles & amphibians of the Hajar Mountains*. Editorial CSIC.

Burriel-Carranza, B., Estarellas, M., Riaño, G., Talavera, A., Tejero-Cicuéndez, H., Els, J., & Carranza, S. (2023a). Species boundaries to the limit: Integrating species delimitation methods is critical to avoid taxonomic inflation in the case of the Hajar Banded Ground Gecko (*Trachydactylus hajarensis*). *Molecular Phylogenetics and Evolution*, *186*, 107834. https://doi.org/10.1016/j.ympev.2023.107834

Burriel-Carranza, B., Mazuch, T., Estarellas, M., Talavera, A., Riaño, G., Koppetsch, T., Tamar, K., Tejero-Cicuéndez, H., Saadi, S. A. l, Busais, S., Kratochvíl, L., Shobrak, M., ŠMíD, J., & Carranza, S. (2023b). *Pristurus guweirensis* Haas, 1943 (Gekkota: Sphaerodactylidae): The most abundant and widely distributed species of *Pristurus* previously referred to as *Pristurus* sp. 1. *Zootaxa*, *5297*, 594–599. https://doi.org/10.11646/zootaxa.5297.4.9

Burriel-Carranza, B., Mochales-Riaño, G., Talavera, A., Els, J., Estarellas, M., Al Saadi, S., Urriago Suarez, J. D., Olsson, P. O., Matschiner, M., & Carranza, S. (2024). Clinging on the brink: Whole genomes reveal human-induced population declines and severe inbreeding in the Critically Endangered Emirati Leaf-toed Gecko (*Asaccus caudivolvulus*). *Molecular Ecology*, *33*, e17451. https://doi.org/10.1111/mec.17451

Burriel-Carranza, B., Koppetsch, T., Tabares, J., Talavera, A., Mochales-Riaño, G., Estarellas, M., Wipfler, B., Els, J., Simó-Riudalbas, M., Adams, D., Al Saadi, S., Garcia-Porta, J., Tamar, K., Šmíd, J., & Carranza, S. (2025a). Cryptic speciation in arid mountains: An integrative revision of the *Pristurus rupestris* species complex (Squamata, Sphaerodactylidae) from Arabia based on morphological, genetic and genomic data, with the description of four new species. *PLoS ONE*, *20*, e0315000. https://doi.org/10.1371/journal.pone.0315000

Burriel-Carranza, B., Tejero-Cicuéndez, H., Carné, A., Mochales-Riaño, G., Talavera, A., Al Saadi, S., Els, J., Šmíd, J., Tamar, K., Tarroso, P., & Carranza, S. (2025b). Integrating genomics and biogeography to unravel the origin of a mountain biota: The case of a reptile endemicity hotspot in Arabia. *Systematic Biology*, *74*, 230–249. https://doi.org/10.1093/sysbio/syae032

Burriel-Carranza, B., Koppetsch, , T., Al-Rashdisaid, , S. H. A., Al-Rahbinasser, , N. N. M. R., Alhashimi, , K. S. S. K., Miró, , G., Estarellas, , M., Tulloch, , S., Piquet, , J., Al Said, , T. A., Al Abdulsalaam, , Z. A., & & Carranza, , S. (2026). New records of the As Sareen Semaphore Gecko (*Pristurus assareen*, Gekkota: Sphaerodactylidae) provide novel insights into the distribution of this microendemic Critically Endangered species. *Zootaxa*, *in press*.

Butchart, S. H. M., Walpole, M., Collen, B., van Strien, A., Scharlemann, J. P. W., Almond, R. E. A., Baillie, J. E. M., Bomhard, B., Brown, C., Bruno, J., Carpenter, K. E., Carr, G. M., Chanson, J., Chenery, A. M., Csirke, J., Davidson, N. C., Dentener, F., Foster, M., Galli, A., … Watson, R. (2010). Global biodiversity: Indicators of recent declines. *Science*, *328*, 1164–1168. https://doi.org/10.1126/science.1187512

Downloaded from https://academic.oup.com/evolut/article/80/6/1311/8660089 by guest on 08 June 2026

Card, D. C., Jennings, W. B., & Edwards, S. V. (2023). Genome evolution and the future of phylogenomics of non-avian reptiles. *Animals*, *13*, 471. https://doi.org/10.3390/ani13030471

Carranza, S., Els, J., & Burriel-Carranza, B. (2021). *A field guide to the reptiles of Oman*. Digital CSIC.

Carter, K., Reyes-Olivares, C., Eubanks, J., Hanna, H., Nielsen, S. V., & Esquerré, D. (2025). Hidden diversity in the driest desert on Earth: Genomics unveils cryptic diversity in an ancient South American gecko lineage (Phyllodactylidae, *Garthia*). *Molecular Phylogenetics and Evolution*, *213*, 108448. https://doi.org/10.1016/j.ympev.2025.108448

Cerca, J., Meyer, C., Stateczny, D., Siemon, D., Wegbrod, J., Purschke, G., Dimitrov, D., & Struck, T. H. (2020). Deceleration of morphological evolution in a cryptic species complex and its link to paleontological stasis. *Evolution*, *74*(1), 116–131. https://doi.org/10.1111/evo.13884

Challis, R., Richards, E., Rajan, J., Cochrane, G., & Blaxter, M. (2020). BlobToolKit—Interactive quality assessment of genome assemblies. *G3 Genes*, *10*, 1361–1374. https://doi.org/10.1534/g3.119.400908

Chan, K. O., Neokleous, D. N., Anuar, S., Brown, R. M., Hutter, C. R., Das, I., & Hertwig, S. T. (2026). A genomic perspective on cryptic species reveals complex evolutionary dynamics in the gray zone of the speciation continuum. *Systematic Biology*, syag001. https://doi.org/10.1093/sysbio/syag001

Chen, S., Zhou, Y., Chen, Y., & Gu, J. (2018). fastp: An ultra-fast all-in-one FASTQ preprocessor. *Bioinformatics*, *34*(17), i884–i890. https://doi.org/10.1093/bioinformatics/bty560

Cheng, H., Concepcion, G. T., Feng, X., Zhang, H., & Li, H. (2021). Haplotype-resolved de novo assembly using phased assembly graphs with hifiasm. *Nature Methods*, *18*(2), 170–175. https://doi.org/10.1038/s41592-020-01056-5

Collyer, M., & Adams, D. C. (2023). RRPP: Linear model evaluation with randomized residuals in a permutation procedure (R package version 2.1.2).

Collyer, M. L., & Adams, D. C. (2013). Phenotypic trajectory analysis: Comparison of shape change patterns in evolution and ecology. *Hystrix, the Italian Journal of Mammalogy*, *24*, 75–83.

Collyer, M. L., & Adams, D. C. (2018). RRPP: An R package for fitting linear models to high-dimensional data using residual randomization. *Methods in Ecology and Evolution*, *9*, 1772–1779. https://doi.org/10.1111/2041-210X.13029

Cox, C. L., & Cox, R. M. (2015). Evolutionary shifts in habitat aridity predict evaporative water loss across squamate reptiles. *Evolution*, *69*(9), 2507–2516. https://doi.org/10.1111/evo.12742

Daza, J. D., Abdala, V., Thomas, R., & Bauer, A. M. (2008). Skull anatomy of the miniaturized gecko *Sphaerodactylus roosevelti* (Squamata: Gekkota). *Journal of Morphology*, *269*, 1340–1364. https://doi.org/10.1002/jmor.10664

Delić, T., Di Batista Borko, Š., Premate, E., Rexhepi, B., Alther, R., Knüsel, M., Malard, F., Weber, D., Stoch, F., Flot, J.-F., Fišer, C., & Altermatt, F. (2025). Phylogenetic origin of morphologically cryptic species shapes co-occurrence and sympatry patterns. *Freshwater Biology*, *70*(2), e70000. https://doi.org/10.1111/fwb.70000

Durant, S. M., Pettorelli, N., Bashir, S., Woodroffe, R., Wacher, T., De Ornellas, P., Ransom, C., Abáigar, T., Abdelgadir, M., El Alqamy, H., Beddiaf, M., Belbachir, F., Belbachir-Bazi, A., Berbash, A. A., Beudels-Jamar, R., Boitani, L., Breitenmoser, C., Cano, M., Chardonnet, P., … Baillie, J. E. M. (2012). Forgotten biodiversity in desert ecosystems. *Science*, *336*(6087), 1379–1380. https://doi.org/10.1126/science.336.6087.1379

Etter, R. J., Rex, M. A., Chase, M. C., & Quattro, J. M. (1999). A genetic dimension to deep-sea biodiversity. *Deep Sea Research Part I: Oceanographic Research Papers*, *46*(7), 1095–1099. https://doi.org/10.1016/S0967-0637(98)00100-9

Feiner, N., Zajac, N., Wen, G., & Uller, T. (2025). Population and evolutionary genomics of lizards and snakes. EcoEvoRxiv,https://doi.org/10.32942/X27Q01

Gabaldón, C., Montero-Pau, J., Serra, M., & Carmona, M. J. (2013). Morphological similarity and ecological overlap in two rotifer species. *PLoS ONE*, *8*, e57087. https://doi.org/10.1371/journal.pone.0057087

Gable, S. M., Mendez, J. M., Bushroe, N. A., Wilson, A., Byars, M. I., & Tollis, M. (2023). The state of squamate genomics: Past, present, and future of genome research in the most speciose terrestrial vertebrate order. *Genes*, *14*, 1387. https://doi.org/10.3390/genes14071387

García-Alcalde, F., Okonechnikov, K., Carbonell, J., Cruz, L. M., Götz, S., Tarazona, S., Dopazo, J., Meyer, T. F., & Conesa, A. (2012). Qualimap: Evaluating next-generation sequencing alignment data. *Bioinformatics*, *28*(20), 2678–2679. https://doi.org/10.1093/bioinformatics/bts503

García-Navas, V., Rodríguez-Rey, M., & Westerman, M. (2018). Bursts of morphological and lineage diversification in modern dasyurids, a 'classic' adaptive radiation. *Biological Journal of the Linnean Society*, *123*, 782–795. https://doi.org/10.1093/biolinnean/bly013

Garcia-Porta, J., Simó-Riudalbas, M., Robinson, M., & Carranza, S. (2017). Diversification in arid mountains: Biogeography and cryptic diversity of *Pristurus rupestris rupestris* in Arabia. *Journal of Biogeography*, *44*, 1694–1704. https://doi.org/10.1111/jbi.12929

Garcia-Porta, J., Šmíd, J., Sol, D., Fasola, M., & Carranza, S. (2016). Testing the island effect on phenotypic diversification: Insights from the *Hemidactylus* geckos of the Socotra Archipelago. *Scientific Reports*, *6*, 23729. https://doi.org/10.1038/srep23729

Gemmell, N. J., Rutherford, K., Prost, S., Tollis, M., Winter, D., Macey, J. R., Adelson, D. L., Suh, A., Bertozzi, T., Grau, J. H., Organ, C., Gardner, P. P., Muffato, M., Patricio, M., Billis, K., Martin, F. J., Flicek, P., Petersen, B., Kang, L., … Edmonds, H. (2020). The tuatara genome reveals ancient features of amniote evolution. *Nature*, *584*, 403–409. https://doi.org/10.1038/s41586-020-2561-9

Graham, M. R., Myers, E. A., Kaiser, R. C., & Fet, V. (2019). Cryptic species and co-diversification in sand scorpions from the Karakum and Kyzylkum deserts of Central Asia. *Zoologica Scripta*, *48*, 801–812. https://doi.org/10.1111/zsc.12381

Grismer, L., Wood, P. L., Poyarkov, N. A., Le, M. D., Karunarathna, S., Chomdej, S., Suwannapoom, C., Qi, S., Liu, S., Che, J., Quah, E. S. H., Kraus, F., Oliver, P. M., Riyanto, A., Pauwels, O. S. G., & Grismer, J. L. (2021b). Karstic landscapes are foci of species diversity in the world's third-largest vertebrate genus *Cyrtodactylus* Gray, 1827 (Reptilia: Squamata; Gekkonidae). *Diversity*, *13*, 183. https://doi.org/10.3390/d13050183

Grismer, L. L., Wood, Jr., P. L., Poyarkov, N. A., Le, M. D., Kraus, F., Agarwal, I., Oliver, P. M., Nguyen, S. N., Nguyen, T. Q., Karunarathna, S., Welton, L. J., Stuart, B. L., Luu, V. Q., Bauer, A. M., O'Connell, K. A., Quah, E. S. H., Chan, K. O., Ziegler, T., Ngo, H., … Grismer, J. L. (2021a). Phylogenetic partitioning of the third-largest vertebrate genus in the world, *Cyrtodactylus* Gray, 1827 (Reptilia; Squamata; Gekkonidae), and its relevance to taxonomy and conservation. *Vertebrate Zoology*, *71*, 101–154. https://doi.org/10.3897/vz.71.e59307

Guan, D., McCarthy, S. A., Wood, J., Howe, K., Wang, Y., & Durbin, R. (2020). Identifying and removing haplotypic duplication in primary genome assemblies. *Bioinformatics*, *36*, 2896–2898. https://doi.org/10.1093/bioinformatics/btaa025

Guarnizo, C. E., Werneck, F. P., Giugliano, L. G., Santos, M. G., Fenker, J., Sousa, L., D'Angiolella, A. B., dos Santos, A. R., Strüssmann, C., Rodrigues, M. T., Dorado-Rodrigues, T. F., Gamble, T., & Colli, G. R. (2016). Cryptic lineages and diversification of an endemic anole lizard (Squamata, Dactyloidae) of the Cerrado hotspot. *Molecular Phylogenetics and Evolution*, *94*, 279–289. https://doi.org/10.1016/j.ympev.2015.09.005

Gunz, P., Mitteroecker, P., Neubauer, S., Weber, G. W., & Bookstein, F. L. (2009). Principles for the virtual reconstruction of hominin crania. *Journal of Human Evolution*, *57*, 48–62. https://doi.org/10.1016/j.jhevol.2009.04.004

Gurevich, A., Saveliev, V., Vyahhi, N., & Tesler, G. (2013). QUAST: Quality assessment tool for genome assemblies. *Bioinformatics*, *29*, 1072–1075. https://doi.org/10.1093/bioinformatics/btt086

Hansman, R. J., Ring, U., Thomson, S. N., den Brok, B., & Stübner, K. (2017). Late Eocene uplift of the Al Hajar Moun-

Downloaded from https://academic.oup.com/evolut/article/80/6/1311/8660089 by guest on 08 June 2026

tains, Oman, supported by stratigraphy and low-temperature thermochronology. *Tectonics*, *36*, 3081–3109. https://doi.org/10.1002/2017TC004672

Herrel, A., De Grauw, E. d, & Lemos-Espinal, J. A. (2001). Head shape and bite performance in xenosaurid lizards. *Journal of Experimental Zoology*, *290*, 101–107. https://doi.org/10.1002/jez.1039

Jörger, K. M., & Schrödl, M. (2013). How to describe a cryptic species? Practical challenges of molecular taxonomy. *Frontiers in Zoology*, *10*, 59. https://doi.org/10.1186/1742-9994-10-59

Kaliontzopoulou, A., Adams, D. C., van der Meijden, A., Perera, A., & Carretero, M. A. (2012). Relationships between head morphology, bite performance and ecology in two species of *Podarcis* wall lizards. *Evolutionary Ecology*, *26*, 825–845. https://doi.org/10.1007/s10682-011-9538-y

Kaliontzopoulou, A., Carretero, M. A., & Adams, D. C. (2015). Ecomorphological variation in male and female wall lizards and the macroevolution of sexual dimorphism in relation to habitat use. *Journal of Evolutionary Biology*, *28*, 80–94. https://doi.org/10.1111/jeb.12540

Koppetsch, T., Malinsky, M., & Matschiner, M. (2024). Towards reliable detection of introgression in the presence of among-species rate variation. *Systematic Biology*, *73*, 769–788. https://doi.org/10.1093/sysbio/syae028

Korunes, K. L., & Samuk, K. (2021). pixy: Unbiased estimation of nucleotide diversity and divergence in the presence of missing data. *Molecular Ecology Resources*, *21*, 1359–1368. https://doi.org/10.1111/1755-0998.13326

Lefébure, T., Douady, C. J., Gouy, M., Trontelj, P., Briolay, J., & Gibert, J. (2006). Phylogeography of a subterranean amphipod reveals cryptic diversity and dynamic evolution in extreme environments. *Molecular Ecology*, *15*, 1797–1806. https://doi.org/10.1111/j.1365-294x.2006.02888.x

Li, H. (2011). A statistical framework for SNP calling, mutation discovery, association mapping and population genetical parameter estimation from sequencing data. *Bioinformatics*, *27*, 2987–2993. https://doi.org/10.1093/bioinformatics/btr509

Li, H. (2013). Aligning sequence reads, clone sequences and assembly contigswith BWA-MEM. *arXiv*, *1303*, 3997. https://doi.org/10.48550/arXiv.1303.3997

Li, H. (2018). Minimap2: Pairwise alignment for nucleotide sequences. *Bioinformatics*, *34*, 3094–3100. https://doi.org/10.1093/bioinformatics/bty191

Li, H., Handsaker, B., Wysoker, A., Fennell, T., Ruan, J., Homer, N., Marth, G., Abecasis, G., & Durbin, R., & 1000 Genome Project Data Processing Subgroup. (2009). The sequence alignment/map format and SAMtools. *Bioinformatics*, *25*, 2078–2079. https://doi.org/10.1093/bioinformatics/btp352

Lobón-Rovira, J., Marugán-Lobón, J., Nebreda, S. M., Buckley, D., Stanley, E. L., Köhnk, S., Glaw, F., Conradie, W., & Bauer, A. M. (2024). Adaptive or non-adaptive? Cranial evolution in a radiation of miniaturized day geckos. *BMC Ecology and Evolution*, *24*, 150. https://doi.org/10.1186/s12862-024-02344-w

López-López, A., Hudson, P., & Galián, J. (2016). Islands in the desert: Species delimitation and evolutionary history of *Pseudotetracha* tiger beetles (Coleoptera: Cicindelidae: Megacephalini) from Australian salt lakes. *Molecular Phylogenetics and Evolution*, *101*, 279–285. https://doi.org/10.1016/j.ympev.2016.05.017

Losos, J. B., & Mahler, D. L. (2010). Adaptive radiation: The interaction of ecological opportunity, adaptation, and speciation. In M. A. Bell, D. J. Futuyma, W. F. Eanes, & J. S. Levinton (Eds.), *Evolution after darwin: the first 150 years* (pp. 381–420). Sinauer Associates.

Malinsky, M., Matschiner, M., & Svardal, H. (2021). Dsuite—Fast *D*-statistics and related admixture evidence from VCF files. *Molecular Ecology Resources*, *21*, 584–595. https://doi.org/10.1111/1755-0998.13265

Manni, M., Berkeley, M. R., Seppey, M., Simão, F. A., & Zdobnov, E. M. (2021). BUSCO update: Novel and streamlined workflows along with broader and deeper phylogenetic coverage for scoring of eukaryotic, prokaryotic, and viral genomes. *Molecular Biology and Evolution*, *38*, 4647–4654. https://doi.org/10.1093/molbev/msab199

Marín, A. G., Olave, M., Avila, L. J., Sites, J. W., & Morando, M. (2018). Evidence of body size and shape stasis driven by selection in Patagonian lizards of the *Phymaturus patagonicus* clade (Squamata: Liolaemini). *Molecular Phylogenetics and Evolution*, *129*, 226–241. https://doi.org/10.1016/j.ympev.2018.08.019

Marçais, G., & Kingsford, C. (2011). A fast, lock-free approach for efficient parallel counting of occurrences of k-mers. *Bioinformatics*, *27*, 764–770. https://doi.org/10.1093/bioinformatics/btr011

McDonald, P. J., Fenner, A. L., Torkkola, J., & Oliver, P. M. (2024). Vicars in the desert: Substrate specialisation and paleo-erosion underpin cryptic speciation in an Australian arid-zone lizard lineage (Diplodactylidae: *Diplodactylus*). *Vertebrate Zoology*, *74*, 577–594. https://doi.org/10.3897/vz.74.e128775

McKenna, A., Hanna, M., Banks, E., Sivachenko, A., Cibulskis, K., Kernytsky, A., Garimella, K., Altshuler, D., Gabriel, S., Daly, M., & DePristo, M. A. (2010). The genome analysis toolkit: A MapReduce framework for analyzing next-generation DNA sequencing data. *Genome Research*, *20*, 1297–1303. https://doi.org/10.1101/gr.107524.110

Meier, J. I., Stelkens, R. B., Joyce, D. A., Mwaiko, S., Phiri, N., Schliewen, U. K., Selz, O. M., Wagner, C. E., Katongo, C., & Seehausen, O. (2019). The coincidence of ecological opportunity with hybridization explains rapid adaptive radiation in Lake Mweru cichlid fishes. *Nature Communications*, *10*, 5391. https://doi.org/10.1038/s41467-019-13278-z

Meiri, S., Bauer, A. M., Allison, A., Castro-Herrera, F., Chirio, L., Colli, G., Das, I., Doan, T. M., Glaw, F., Grismer, L. L., Hoogmoed, M., Kraus, F., LeBreton, M., Meirte, D., Nagy, Z. T., Nogueira, C. D. e C., Oliver, P., Pauwels, O. S. G., Pincheira-Donoso, D., … Roll, U. (2018). Extinct, obscure or imaginary: The lizard species with the smallest ranges. *Diversity and Distributions*, *24*(2), 262–273. https://doi.org/10.1111/ddi.12678

Mendes, J., Salvi, D., Harris, D. J., Els, J., & Carranza, S. (2018). Hidden in the Arabian Mountains: Multilocus phylogeny reveals cryptic diversity in the endemic *Omanosaura* lizards. *Journal of Zoological Systematics and Evolutionary Research*, *56*, 395–407. https://doi.org/10.1111/jzs.12210

Minh, B. Q., Schmidt, H. A., Chernomor, O., Schrempf, D., Woodhams, M. D., von Haeseler, A., & Lanfear, R. (2020). IQ-TREE 2: New models and efficient methods for phylogenetic inference in the genomic era. *Molecular Biology and Evolution*, *37*, 1530–1534. https://doi.org/10.1093/molbev/msaa015

Oliver, P. M., & Sanders, K. L. (2009). Molecular evidence for Gondwanan origins of multiple lineages within a diverse Australasian gecko radiation. *Journal of Biogeography*, *36*, 2044–2055. https://doi.org/10.1111/j.1365-2699.2009.02149.x

Openshaw, G. H., & Keogh, J. S. (2014). Head shape evolution in monitor lizards (*Varanus*): Interactions between extreme size disparity, phylogeny and ecology. *Journal of Evolutionary Biology*, *27*, 363–373. https://doi.org/10.1111/jeb.12299

Pedersen, B. S., & Quinlan, A. R. (2018). Mosdepth: Quick coverage calculation for genomes and exomes. *Bioinformatics*, *34*, 867–868. https://doi.org/10.1093/bioinformatics/btx699

Pianka, E. R. (1989). Desert lizard diversity: Additional comments and some data. *The American Naturalist*, *134*, 344–364. https://doi.org/10.1086/284985

Pinto, B. J., Gamble, T., Smith, C. H., & Wilson, M. A. (2023). A lizard is never late: Squamate genomics as a recent catalyst for understanding sex chromosome and microchromosome evolution. *Journal of Heredity*, *114*, 445–458. https://doi.org/10.1093/jhered/esad023

Prates, I., Hutchinson, M. N., Singhal, S., Moritz, C., & Rabosky, D. L. (2024). Notes from the taxonomic disaster zone: Evolutionary drivers of intractable species boundaries in an Australian lizard clade (Scincidae: *Ctenotus*). *Molecular Ecology*, *33*, e17074. https://doi.org/10.1111/mec.17074

Rambaut, A., Drummond, A. J., Xie, D., Baele, G., & Suchard, M. A. (2018). Posterior summarization in Bayesian phylogenetics using

Downloaded from https://academic.oup.com/evolut/article/80/6/1311/8660089 by guest on 08 June 2026

Tracer 1.7. *Systematic Biology*, *67*, 901–904. https://doi.org/10.1093/sysbio/syy032

Ranallo-Benavidez, T. R., Jaron, K. S., & Schatz, M. C. (2020). GenomeScope 2.0 and Smudgeplot for reference-free profiling of polyploid genomes. *Nature Communications*, *11*, 1432. https://doi.org/10.1038/s41467-020-14998-3

Rhie, A., McCarthy, S. A., Fedrigo, O., Damas, J., Formenti, G., Koren, S., Uliano-Silva, M., Chow, W., Fungtammasan, A., Kim, J., Lee, C., Ko, B. J., Chaisson, M., Gedman, G. L., Cantin, L. J., Thibaud-Nissen, F., Haggerty, L., Bista, I., Smith, M., … Jarvis, E. D. (2021). Towards complete and error-free genome assemblies of all vertebrate species. *Nature*, *592*, 737–746. https://doi.org/10.1038/s41586-021-03451-0

Rhie, A., Walenz, B. P., Koren, S., & Phillippy, A. M. (2020). Merqury: Reference-free quality, completeness, and phasing assessment for genome assemblies. *Genome Biology*, *21*, 245. https://doi.org/10.1186/s13059-020-02134-9

Rieppel, O. (1984). Miniaturization of the lizard skull: Its functional and evolutionary implications. In M. Ferguson (Ed.), *The structure, development and evolution of reptiles* (pp. 503–520). Academic Press.

Roll, U., Feldman, A., Novosolov, M., Allison, A., Bauer, A. M., Bernard, R., Böhm, M., Castro-Herrera, F., Chirio, L., Collen, B., Colli, G. R., Dabool, L., Das, I., Doan, T. M., Grismer, L. L., Hoogmoed, M., Itescu, Y., Kraus, F., LeBreton, M., … Meiri, S. (2017). The global distribution of tetrapods reveals a need for targeted reptile conservation. *Nature Ecology & Evolution*, *1*, 1677–1682. https://doi.org/10.1038/s41559-017-0332-2

Ronco, F., Matschiner, M., Böhne, A., Boila, A., Büscher, H. H., El Taher, A., Indermaur, A., Malinsky, M., Ricci, V., Kahmen, A., Jentoft, S., & Salzburger, W. (2021). Drivers and dynamics of a massive adaptive radiation in cichlid fishes. *Nature*, *589*, 76–81. https://doi.org/10.1038/s41586-020-2930-4

Rubinoff, D., Reil, J. B., Osborne, K. H., Gregory, C. J., Geib, S. M., & Dupuis, J. R. (2020). Phylogenomics reveals conservation challenges and opportunities for cryptic endangered species in a rapidly disappearing desert ecosystem. *Biodiversity and Conservation*, *29*, 2185–2200. https://doi.org/10.1007/s10531-020-01968-w

Schembri, R., Bromham, L., Moritz, C., & Hua, X. (2025). Comparing rates of molecular and morphological evolution identifies multiple speciation trajectories in a diverse radiation of skinks. *Evolution*, *79*(5), 858–868. https://doi.org/10.1093/evolut/qpaf033

Schield, D. R., Adams, R. H., Card, D. C., Corbin, A. B., Jezkova, T., Hales, N. R., Meik, J. M., Perry, B. W., Spencer, C. L., Smith, L. L., García, G. C., Bouzid, N. M., Strickland, J. L., Parkinson, C. L., Borja, M., Castañeda-Gaytán, G., Bryson, R. W., Flores-Villela, O. A., Mackessy, S. P., … Castoe, T. A. (2018). Cryptic genetic diversity, population structure, and gene flow in the Mojave rattlesnake (*Crotalus scutulatus*). *Molecular Phylogenetics and Evolution*, *127*, 669–681. https://doi.org/10.1016/j.ympev.2018.06.013

Scriven, J. J., Whitehorn, P. R., Goulson, D., & Tinsley, M. C. (2016). Niche partitioning in a sympatric cryptic species complex. *Ecology and Evolution*, *6*, 1328–1339. https://doi.org/10.1002/ece3.1965

Simó-Riudalbas, M., Metallinou, M., de Pous, P., Els, J., Jayasinghe, S., Péntek-Zakar, E., Wilms, T., Al-Saadi, S., & Carranza, S. (2017). Cryptic diversity in *Ptyodactylus* (Reptilia: Gekkonidae) from the northern Hajar Mountains of Oman and the United Arab Emirates uncovered by an integrative taxonomic approach. *PLoS ONE*, *12*, e0180397. https://doi.org/10.1371/journal.pone.0180397

Simó-Riudalbas, M., Tarroso, P., Papenfuss, T., Al-Sariri, T., & Carranza, S. (2018). Systematics, biogeography and evolution of *Asaccus gallagheri* (Squamata, Phyllodactylidae) with the description of a new endemic species from Oman. *Systematics and Biodiversity*, *16*(4), 323–339. https://doi.org/10.1080/14772000.2017.1403496

Skipwith, P. L., Bauer, A. M., Jackman, T. R., & Sadlier, R. A. (2016). Old but not ancient: Coalescent species tree of New Caledonian geckos reveals recent post-inundation diversification. *Journal of Biogeography*, *43*, 1266–1276. https://doi.org/10.1111/jbi.12719

Šmíd, J., Sindaco, R., Shobrak, M., Busais, S., Tamar, K., Aghová, T., Simó-Riudalbas, M., Tarroso, P., Geniez, P., Crochet, P.-A., Els, J., Burriel-Carranza, B., Tejero-Cicuéndez, H., & Carranza, S. (2021). Diversity patterns and evolutionary history of Arabian squamates. *Journal of Biogeography*, *48*, 1183–1199. https://doi.org/10.1111/jbi.14070

Smith, K. L., Harmon, L. J., Shoo, L. P., & Melville, J. (2011). Evidence of constrained phenotypic evolution in a cryptic species complex of agamid lizards: Phenotypic stability in a cryptic radiation of Australian lizards. *Evolution*, *65*, 976–992. https://doi.org/10.1111/j.1558-5646.2010.01211.x

Solís-Lemus, C., & Ané, C. (2016). Inferring phylogenetic networks with maximum pseudolikelihood under incomplete lineage sorting. *PLoS Genetics*, *12*, e1005896. https://doi.org/10.1371/journal.pgen.1005896

Stange, M., Sánchez-Villagra, M. R., Salzburger, W., & Matschiner, M. (2018). Bayesian divergence-time estimation with genome-wide single-nucleotide polymorphism data of sea catfishes (Ariidae) supports Miocene closure of the Panamanian Isthmus. *Systematic Biology*, *67*, 681–699. https://doi.org/10.1093/sysbio/syy006

Stroud, J. T., & Losos, J. B. (2016). Ecological opportunity and adaptive radiation. *Annual Review of Ecology, Evolution, and Systematics*, *47*, 507–532. https://doi.org/10.1146/annurev-ecolsys-121415-032254

Struck, T. H., Feder, J. L., Bendiksby, M., Birkeland, S., Cerca, J., Gusarov, V. I., Kistenich, S., Larsson, K.-H., Liow, L. H., Nowak, M. D., Stedje, B., Bachmann, L., & Dimitrov, D. (2018). Finding evolutionary processes hidden in cryptic species. *Trends in Ecology & Evolution*, *33*, 153–163. https://doi.org/10.1016/j.tree.2017.11.007

Tamar, K., Chirio, L., Shobrak, M., Busais, S., & Carranza, S. (2019a). Using multilocus approach to uncover cryptic diversity within *Pseudotrapelus* lizards from Saudi Arabia. *Saudi Journal of Biological Sciences*, *26*, 1442–1449. https://doi.org/10.1016/j.sjbs.2019.05.006

Tamar, K., Mitsi, P., & Carranza, S. (2019b). Cryptic diversity revealed in the leaf-toed gecko *Asaccus montanus* (Squamata, Phyllodactylidae) from the Hajar Mountains of Arabia. *Journal of Zoological Systematics and Evolutionary Research*, *57*, 369–382. https://doi.org/10.1111/jzs.12258

Tejero-Cicuéndez, H., Menéndez, I., Talavera, A., Mochales-Riaño, G., Burriel-Carranza, B., Simó-Riudalbas, M., Carranza, S., & Adams, D. C. (2023). Evolution along allometric lines of least resistance: Morphological differentiation in *Pristurus* geckos. *Evolution*, *77*, 2547–2560. https://doi.org/10.1093/evolut/qpad166

Tejero-Cicuéndez, H., Simó-Riudalbas, M., Menéndez, I., & Carranza, S. (2021). Ecological specialization, rather than the island effect, explains morphological diversification in an ancient radiation of geckos. *Proceedings of the Royal Society B*, *288*, 20211821. https://doi.org/10.1098/rspb.2021.1821

Tejero-Cicuéndez, H., Tarroso, P., Carranza, S., & Rabosky, D. L. (2022). Desert lizard diversity worldwide: Effects of environment, time, and evolutionary rate. *Global Ecology and Biogeography*, *31*, 776–790. https://doi.org/10.1111/geb.13470

Tobler, M., Palacios, M., Chapman, L. J., Mitrofanov, I., Bierbach, D., Plath, M., Arias-Rodriguez, L., García de León, F. J., & Mateos, M. (2011). Evolution in extreme environments: Replicated phenotypic differentiation in livebearing fish inhabiting sulfidic springs. *Evolution*, *65*, 2213–2228. https://doi.org/10.1111/j.1558-5646.2011.01298.x

Uetz, P., Freed, P., Aguilar, R., Reyes, F., Kudera, J., & Hošek, J. (2025). The reptile database. http://www.reptiledatabase.org

Vasimuddin, M. d., Misra, S., Li, H., & Aluru, S. (2019). Efficient architecture-aware acceleration of BWA-MEM for multicore systems. In *2019 IEEE international parallel and distributed processing symposium (IPDPS)* (pp. 314–324). IEEE.

Verwaijen, D., Van Damme, R., & Herrel, A. (2002). Relationships between head size, bite force, prey handling efficiency and diet in

Downloaded from https://academic.oup.com/evolut/article/80/6/1311/8660089 by guest on 08 June 2026

two sympatric lacertid lizards. *Functional Ecology*, *16*, 842–850. https://doi.org/10.1046/j.1365-2435.2002.00696.x

Vrijenhoek, R. C., Schutz, S. J., Gustafson, R. G., & Lutz, R. A. (1994). Cryptic species of deep-sea clams (Mollusca: Bivalvia: Vesicomyidae) from hydrothermal vent and cold-water seep environments. *Deep Sea Research Part I: Oceanographic Research Papers*, *41*, 1171–1189. https://doi.org/10.1016/0967-0637(94)90039-6

Warheit, K. I., Forman, J. D., Losos, J. B., & Miles, D. B. (1999). Morphological diversification and adaptive radiation: A comparison of two diverse lizard clades. *Evolution*, *53*, 1226–1234. https://doi.org/10.1111/j.1558-5646.1999.tb04535.x

Wellborn, G. A., & Langerhans, R. B. (2015). Ecological opportunity and the adaptive diversification of lineages. *Ecology and Evolution*, *5*, 176–195. https://doi.org/10.1002/ece3.1347

Zhang, Y., & Wiens, J. J. (2026). Cryptic species are widespread across vertebrates. *Proceedings of the Royal Society B*, *293*, 20252377. https://doi.org/10.1098/rspb.2025.2377

Downloaded from https://academic.oup.com/evolut/article/80/6/1311/8660089 by guest on 08 June 2026

Received October 1, 2025; revisions received March 20, 2026; accepted March 27, 2026
Associate Editor: Antigoni Kaliontzopoulou; Handling Editor: Hélène Morlon
© The Author(s) 2026. Published by Oxford University Press on behalf of The Society for the Study of Evolution (SSE). This is an Open Access article distributed under the terms of the Creative Commons Attribution License (https://creativecommons.org/licenses/by/4.0/), which permits unrestricted reuse, distribution, and reproduction in any medium, provided the original work is properly cited.